

## INFORMATION TO USERS

This material was produced from a microfilm copy of the original document. While the most advanced technological means to photograph and reproduce this document have been used, the quality is heavily dependent upon the quality of the original submitted.

The following explanation of techniques is provided to help you understand markings or patterns which may appear on this reproduction.

1. The sign or "target" for pages apparently lacking from the document photographed is "Missing Page(s)". If it was possible to obtain the missing page(s) or section, they are spliced into the film along with adjacent pages. This may have necessitated cutting thru an image and duplicating adjacent pages to insure you complete continuity.
2. When an image on the film is obliterated with a large round black mark, it is an indication that the photographer suspected that the copy may have moved during exposure and thus cause a blurred image. You will find a good image of the page in the adjacent frame.
3. When a map, drawing or chart, etc., was part of the material being photographed the photographer followed a definite method in "sectioning" the material. It is customary to begin photoing at the upper left hand corner of a large sheet and to continue photoing from left to right in equal sections with a small overlap. If necessary, sectioning is continued again — beginning below the first row and continuing on until complete.
4. The majority of users indicate that the textual content is of greatest value, however, a somewhat higher quality reproduction could be made from "photographs" if essential to the understanding of the dissertation. Silver prints of "photographs" may be ordered at additional charge by writing the Order Department, giving the catalog number, title, author and specific pages you wish reproduced.
5. PLEASE NOTE: Some pages may have indistinct print. Filmed as received.

### University Microfilms International

300 North Zeeb Road  
Ann Arbor, Michigan 48106 USA  
St. John's Road, Tyler's Green  
High Wycombe, Bucks, England HP10 8HR

77-29,514

FERREIRA, Paulo Afonso, 1938-  
EVAPOTRANSPIRATION AND SOIL MATRIC POTENTIALS  
USING TENSION IRRIGATION.

The University of Arizona, Ph.D., 1977  
Engineering, agricultural

**Xerox University Microfilms**, Ann Arbor, Michigan 48106

EVAPOTRANSPIRATION AND SOIL MATRIC POTENTIALS  
USING TENSION IRRIGATION

by

Paulo Afonso Ferreira

---

A Dissertation Submitted to the Faculty of the  
DEPARTMENT OF SOILS, WATER AND ENGINEERING  
In Partial Fulfillment of the Requirements  
For the Degree of  
DOCTOR OF PHILOSOPHY  
WITH A MAJOR IN SOIL AND WATER SCIENCE  
In the Graduate College  
THE UNIVERSITY OF ARIZONA

1 9 7 7

THE UNIVERSITY OF ARIZONA

GRADUATE COLLEGE

I hereby recommend that this dissertation prepared under my  
direction by Paulo Afonso Ferreira  
entitled Evapotranspiration and Soil Matric Potentials  
Using Tension Irrigation  
be accepted as fulfilling the dissertation requirement for the  
degree of Doctor of Philosophy

*D. P. Langmeier*  
Dissertation Director

July 29, 1977  
Date

As members of the Final Examination Committee, we certify  
that we have read this dissertation and agree that it may be  
presented for final defense.

*A. H. Kovich*  
*T. K. O'Connell*  
*Robert A. Smith*  
Allan D. Halderman  
*W. J. Matlock*

Aug. 1, 1977  
8-1-77  
8-1-77  
~~8/22/77~~ <sup>ADH</sup> 8/1/77  
8/1/77

Final approval and acceptance of this dissertation is contingent  
on the candidate's adequate performance and defense thereof at the  
final oral examination.

STATEMENT BY AUTHOR

This dissertation has been submitted in partial fulfillment of requirements for an advanced degree at The University of Arizona and is deposited in the University Library to be made available to borrowers under rules of the Library.

Brief quotations from this dissertation are allowable without special permission, provided that accurate acknowledgment of source is made. Requests for permission for extended quotation from or reproduction of this manuscript in whole or in part may be granted by the head of the major department or the Dean of the Graduate College when in his judgment the proposed use of the material is in the interests of scholarship. In all other instances, however, permission must be obtained from the author.

SIGNED:

Paulo Honorio Ferreira

To my wife, Maria Celia, and  
children, Renata, Ana Paula, and Lucille.

## ACKNOWLEDGMENTS

The author wishes to express his deepest appreciation and sincere gratitude to his major professor, Dr. D. D. Fangmeier, for his helpful guidance, encouragement, and suggestions throughout this study and during the writing of this dissertation.

Appreciation is also extended to Dr. A. W. Warrick, Dr. G. R. Dutt, Dr. W. G. Matlock, Mr. A. D. Halderman, and Dr. R. K. Frevert for their assistance during this program and constructive criticism in correcting the manuscript.

The author is especially grateful to Dr. A. W. Warrick for his invaluable ideas and suggestions throughout the development and application of the mathematical models to my research.

And a special note of thanks to all faculty members, graduate students, and employees of the Soils, Water and Engineering Department, and many friends, who made my stay in this country a valuable and memorable experience.

Grateful acknowledgment is also extended to the Federal University of Vicosa and the United States Department of Agriculture for the financial support and help which made these studies possible.

## TABLE OF CONTENTS

	Page
LIST OF ILLUSTRATIONS . . . . .	vii
LIST OF TABLES . . . . .	ix
ABSTRACT . . . . .	x
1. INTRODUCTION . . . . .	1
2. LITERATURE REVIEW . . . . .	3
Negative Head Irrigation . . . . .	3
Lettuce Water Use . . . . .	5
Unsaturated Hydraulic Conductivity . . . . .	7
Mathematical Modeling of Soil-Water Movement . . . . .	9
3. EQUIPMENT AND PROCEDURE . . . . .	14
Equipment and Experimental Setup . . . . .	14
Procedure . . . . .	16
Soil Preparation and Packing . . . . .	16
Lettuce Planting, Thinning, and Nitrogen Application . . . . .	18
Treatments . . . . .	18
Intake Control and Measurements . . . . .	19
4. RESULTS AND DISCUSSION . . . . .	20
Evapotranspiration . . . . .	20
Fall Experiment . . . . .	20
Winter Experiment . . . . .	24
Hydraulic Conductivity of Soil . . . . .	29
Measured Soil Matric Potentials . . . . .	32
Flow Resistance and Change in the Negative Head . . . . .	32
Lettuce Yield . . . . .	36
5. COMPARISONS OF CALCULATED AND MEASURED SOIL MATRIC POTENTIALS . . . . .	38
One-Dimensional Soil-Moisture Model . . . . .	38
Plane Sink . . . . .	39
Plane Source . . . . .	41
Infiltration Model . . . . .	42

TABLE OF CONTENTS--Continued

	Page
Numerical Calculations . . . . .	43
Fall Experiment . . . . .	43
Winter Experiment . . . . .	49
6. TENSION IRRIGATION DESIGN CRITERIA . . . . .	56
Example 1 . . . . .	56
Example 2 . . . . .	61
Placement of the Line Sources . . . . .	62
7. SUMMARY AND CONCLUSIONS . . . . .	68
APPENDIX: MEASURED VALUES OF EVAPOTRANSPIRATION AND SOIL MATIC POTENTIALS FOR THE FALL AND WINTER EXPERIMENTS . . . .	72
LITERATURE CITED . . . . .	81

## LIST OF ILLUSTRATIONS

Figure	Page
1. Flux versus Hydraulic Head Relationship for the Ceramic Tubes . . . . .	15
2. Experimental Setup . . . . .	17
3. Daily Average Temperature and Evapotranspiration for the Fall Experiment . . . . .	21
4. Daily Average Relative Humidity . . . . .	23
5. Cumulative Evapotranspiration for the Fall Experiment . . .	25
6. Daily Average Temperature and Evapotranspiration for the Winter Experiment -- Treatment I . . . . .	26
7. Daily Average Temperature and Evapotranspiration for the Winter Experiment -- Treatment II . . . . .	27
8. Daily Average Temperature and Evapotranspiration for the Winter Experiment -- Treatment III . . . . .	28
9. Cumulative Evapotranspiration for the Winter Experiment . .	30
10. Moisture Characteristic Curve for Pima Clay Loam . . . . .	31
11. Hydraulic Conductivity and Volumetric Water Content Relationship for Pima Clay Loam . . . . .	33
12. Hydraulic Conductivity and Pressure Head Relationship for Pima Clay Loam . . . . .	34
13. Geometry of the Flow Problem . . . . .	40
14. Hydraulic Conductivity and Capillary Potential Relationship for Pima Clay Loam . . . . .	44
15. Comparison of the Predicted and Measured Pressure Head for Uniform and Non-Uniform Water Withdrawal Patterns for the Fall Experiment . . . . .	46
16. Uptake Pattern . . . . .	47

LIST OF ILLUSTRATIONS--Continued

Figure		Page
17.	Comparison of the Predicted and Measured Pressure Head for the Winter Experiment -- Treatment I . . . . .	51
18.	Comparison of the Predicted and Measured Pressure Head for the Winter Experiment -- Treatment II . . . . .	52
19.	Comparison of the Predicted and Measured Pressure Head for the Winter Experiment -- Treatment III . . . . .	53
20.	Profile of the Matric Flux Potential and Hydraulic Conductivity . . . . .	55
21.	Two-Dimensional Matric Flux Potential Distribution without Sink . . . . .	64
22.	Predicted Matric Flux Potential and Pressure Head without Sink . . . . .	66
23.	Predicted Matric Flux Potential and Pressure Head with Sink . . . . .	67

LIST OF TABLES

Table		Page
1.	Twenty-Day Average of Soil Matric Potentials for the Fall and Winter Experiments . . . . .	35
2.	Lettuce Yield for Fall and Winter Experiments . . . . .	37
3.	Calculated Matric Flux Potentials, Capillary Potentials, and $K(=\alpha\phi)$ as a Function of $Z/L$ . . . . .	50
4.	Dimensionless Matric Flux Potential at Plane Source Depth . .	57
5.	Input Parameters for Examples 1 and 2 . . . . .	58
6.	Values of the Matric Flux Potential and Pressure Head versus Depth for Example 1 . . . . .	60

## ABSTRACT

Lettuce (Lactuca sativa L.) was raised in a greenhouse during the Fall and Winter seasons 1976-1977, under controlled soil matric potentials, using a tension irrigation system. The tension irrigation system consisted of a soil bin (45 cm deep, 55 cm long, and 30.5 cm wide) and four ceramic tubes buried at 18 cm and connected to a negative head water delivery system by plastic tubing. Soil matric potentials were measured at the 8, 18 (source depth), 29, and 39 cm depths. Air temperature and relative humidity were continuously recorded by a hygrothermograph placed near the soil bins.

The soil material was a Pima clay loam obtained from the University of Arizona experimental farm at Marana. Lettuce plants were thinned to two plants per soil bin which is equivalent to one plant per 839 cm<sup>2</sup>. The consumptive use of water by lettuce was measured by direct readings from the water delivery system reservoir. The evapotranspiration rate for the Fall experiment increased during the first 50 days of growth, corresponding to the increase in leaf area. Maximum values recorded were 4.2 mm/day and the total water used was 240 mm.

The Winter experiment consisted of three soil-water treatments: Treatment I, -10 to -15 cbars soil matric potential during the growing season; Treatment II, -10 to -15 cbars during the first 45 days of growth and then -20 to -25 cbars; and Treatment III, -10 to -15 cbars during the first 45 days of growth and then -30 to -35 cbars. The three treatments

had similar evapotranspiration rates during the first 45 days of the growing season. With adjustment of the soil matric potentials, a tendency of increasing evapotranspiration rates at higher soil water potential was observed. Oscillation of the daily evapotranspiration data revealed a capacity of the tension irrigation system to meet the consumptive use of water by plants. Maximum evapotranspiration rates were 7.0, 4.9, and 4.4 mm/day for Treatments I, II, and III, respectively. The corresponding total water used was 206, 188, and 174 mm.

A one-dimensional soil-moisture model was developed and measured values of the soil matric potentials were compared with predicted values. For the Fall experiment, an adequate agreement between calculated and measured soil-water potential was achieved by assuming 60 percent of the water was withdrawn from the top 22 cm of the root zone and 40 percent withdrawn below. Predicted soil matric potentials were within 12 percent of the measured values.

A uniform water withdrawal pattern by the plants resulted in good agreement between measured and predicted soil matric potentials for the Winter experiment. Exceptions were the 29 cm depth of Treatments II and III and the 39 cm depth of Treatment I where the computed soil matric potentials were within 21 percent of the measured values. A high root density just below the source and poor simulation of the lower boundary condition by the mathematical model were assumed to be the main reasons for the poor agreement at these points.

Tension irrigation system design criteria based on the values of the dimensionless matric flux potential at the plane source depth are presented.

## CHAPTER 1

### INTRODUCTION

Increasing demand for food and fiber as well as limited water supplies requires irrigated agriculture to produce more with less water. Improving the use of water resources and determining the optimum amount of water to be applied to a given irrigated field have been the subjects of many research efforts. Improving the efficiency of surface irrigation systems and using sprinkler or trickle systems have been and are being evaluated as means for reducing the water requirements of irrigated agriculture.

Subsurface irrigation has been tried with success under certain conditions. Some crops can be grown without reduction in yield and quality using less water than by traditional methods. One new specific form of subsurface irrigation is called tension irrigation.

Tension irrigation is the continuous delivery of water under a negative head through buried porous tubes. Soil moisture tension in the plant root zone causes water to move from a water supply through the tube and into the soil. The flow rate is proportional to the soil moisture tension which depends on evaporation and transpiration rates.

A tension irrigation system can be used as a research tool to measure evapotranspiration and the effects of different soil moisture tensions on plant growth if management practices and design criteria can be developed. Prerequisites to proper tension irrigation design are a

basic understanding of unsaturated soil-water movement, soil moisture extraction pattern of the irrigated crop, soil moisture levels to be maintained during the growing season, and the amount of available water that can be stored in the soil profile.

The objectives of this study were: (1) to measure evapotranspiration and growth response of lettuce (Lactuca sativa L.) to three different soil moisture tensions using a tension irrigation system; (2) to compare measured soil matric potentials with values calculated from an analytical solution of the one-dimension soil moisture equation; and (3) to develop criteria for tension irrigation system design based on soil moisture patterns and plant response.

## CHAPTER 2

### LITERATURE REVIEW

#### Negative Head Irrigation

A feasible method for controlling soil-water tension under growing plants would be of particular value for those interested in growing plants under uniform conditions. Researchers may wish to study the effect of changing soil moisture on plant growth or even to observe the effect of different fertilizer application levels under a uniform soil moisture tension. Livingston (1908) first suggested using a porous clay cup buried in a soil-filled pot to maintain a constant soil-water potential. As water is removed from the soil by evapotranspiration, the capillary equilibrium between the soil-water and the water within the porous porcelain is disturbed and water moves from the supply into the soil. When the soil loses water it usually shrinks, and when the lost water is replaced the resulting swelling often fails to bring the soil mass back to exactly the form that it had before. The importance of an adequate capillary continuity between the water of the soil and that of the porous porcelain to the rate of water movement was recognized by Livingston (1918), who suggested using a porous clay cone placed vertically in the center of the pot or even to install cylindrical cones in an oblique or horizontal position as an improvement of the first "auto-irrigator." Tensions up to 40 cm of mercury were used experimentally by Livingston, Hemmi, and Wilson (1926) for sandy, loamy, and humus soils.

They found that, for any soil, there is a certain range of soil-water contents and corresponding water intake rates that can be established and maintained by the tension system through the growing season. The lower limit of this range was lower for sandy soil and higher for clays and humus soils. Tensions of 60 to 65 cm of mercury were considered to be maximum for satisfactory performance of the system. When working in a range of high soil-water tension, plant roots may become massed around the surface of the porous ceramic material and the soil becomes dry a few centimeters from the water source, as observed by Hendrickson and Veihmeyer (1931).

A substantial improvement in apparatus design for better water distribution was made with the development of double-walled irrigator pots with space for water between the glazed outer wall and the porous inner wall (Wilson, 1929; Richards and Blood, 1934). Richards and Loomis (1942) found that even this improvement cannot always supply enough water to maintain uniform soil moisture for rapidly transpiring plants and they reported total failure of the system for water supply tensions of 8.0 and 14.0 cm of mercury and reasonably good control for 2.0 cm of mercury. However, Read, Fleck, and Pelton (1962) reported successful use of "auto-irrigators" to maintain a constant matric potential for a negative head of 50 cm of water. They used a porous cylinder 6 inches long and 1-1/2 inches in diameter installed vertically in the center of the pot. Soil moisture potential was maintained within  $\pm 10$  cm during a 60-day period of growth.

### Lettuce Water Use

Lettuce requires as uniform a soil moisture content during the growing season as is practically possible to maintain. Abrupt fluctuations in soil moisture, mainly in the early and late stages of growth, are detrimental to regular plant development (Whitaker et al., 1974). The soil moisture supply should be adequate but not excessive. Schwalen and Wharton (1930) believed that both yield and quality of head lettuce are improved when high soil moisture is uniformly maintained throughout the growing season for either the Winter or Spring crop. However, Wharton and Hobart (1931) remarked that the presence of excess moisture above the field capacity of the soil retarded root development and growth of the lettuce plant due to poor soil aeration. On a New York peat soil with a high water table, Knott, Andersen and Sweet (1939) found that, when the water supply was excessive, lettuce growth was stunted and heading was delayed and poor.

Stanhill (1957, p. 210) reported that Majmudar, who used tensiometers for soil moisture control, did not find significant differences among lettuce plants subjected to different soil moisture regimes. On the other hand, Taylor and Ashcroft (1972, p. 421) depicted results of Bierhuizen, who raised lettuce during two different seasons, Spring and Fall, in a greenhouse experiment. Bierhuizen's results showed a gain in fresh weight with increasing soil matric potential up to a limiting value of about -20 joules/kg (i.e., about -200 cm of water).

The total amount of water applied for a successful lettuce crop is highly dependent on soil type, growing season, salinity status of the

soil and irrigation water. Veihmeyer and Holland (1949) concluded that, under good irrigation practice, a total of about 14 inches of water is enough to produce a Summer or Fall lettuce crop. An average consumptive use of 8.5 inches of water by lettuce was estimated by Erie, French, and Harris (1968). They determined the consumptive use of water by gravimetric soil moisture measurement techniques. The soil was sampled by depths and locations that were expected to best evaluate the average soil moisture distribution and depletion by the plants under study. Also, the seasonal use in inches per foot and percentage of the total water used was included. Robinson (1970) found that 14 inches of water were adequate for lettuce plant needs and leaching of salts. He applied a depth of water equivalent to that evaporated from a Class A, U. S. Weather Bureau Evaporation Pan. Studies of evapotranspiration of head lettuce on three soil types at an elevation of about 7600 ft above sea level were conducted by Moore and Soltanpour (1972). An average evapotranspiration (Eta) of  $19.3 \pm 6.7$  inches was reported for an 85-day growing season. The average Class A pan evaporation (Epan) was 22.1 inches, resulting in a Eta/Epan ratio of 0.87.

Root depth is an important parameter for good irrigation management. The root system of most head lettuce cultivars can extend to depths of 65 cm or more. However, the root density at this depth is relatively small and the plants are maintained primarily from roots concentrated in the first 35 cm of the soil profile (Whitaker et al., 1974). Therefore, small, frequent water applications would be more advantageous than heavy, infrequent applications.

The use of sprinkler irrigation has increased in popularity, especially for germination and seedling emergence. It presents advantages over furrow irrigation in preventing salt accumulation on the surface of the beds near the germinating seeds, uniform application of water, cooling of the soil surface, better soil aeration, and significantly lower water requirement. Use of sprinkler irrigation for the entire season had a favorable effect on other cultural practice as reported by Robinson (1970). However, growers in Arizona have had problems with the lettuce disease sclerotinia associated with sprinkler irrigation during the entire season.

#### Unsaturated Hydraulic Conductivity

The validity of Darcy's law for the flux of liquid water in unsaturated media has long been assumed. Investigations carried out by Richards (1931), Moore (1939), Childs and Collis-George (1950), and others confirm that Darcy's law for unsaturated flow can be written as  $v = K(\theta)i$ . The left term is a flux called the Darcy velocity (units L/T);  $K(\theta)$  is the unsaturated hydraulic conductivity (units L/T) which depends on the volumetric water content,  $\theta$  (dimensionless); and  $i$  is the hydraulic gradient (dimensionless). The unsaturated hydraulic conductivity,  $K(\theta)$ , is reported to decrease very rapidly as  $\theta$  decreases from its saturation value. The following reasons explain the abrupt decrease in  $K(\theta)$  with  $\theta$ : the total cross-section available for flow decreases, the largest pores are emptied first, and, in the case of drier ranges, there is an increasing probability that the water occurs in pores and wedges isolated from continuous water films and channels (Philip, 1957).

The correlation of both saturated and unsaturated hydraulic conductivity values of a homogeneous porous media to pore-size distribution data has been the subject of many studies. Childs and Collis-George (1950) proposed a theory wherein the flow is determined by the pore radii and by the probability of continuity of pores of different radii in adjacent planes. The disadvantage of the method is the complexity of calculation. Marshall (1958), using arbitrary equal volume components of the porosity, proposed a simpler expression for  $K(\theta)$ . Based on the theory of pore interaction, Millington and Quirk (1959, 1960, 1961) greatly improved the pore-size distribution model.

Laboratory-measured conductivity values were compared with the results of the above methods by Jackson, Reginato, and Van Bavel (1965). They found that the Millington-Quirk method gave good results on disturbed samples, when matched at the saturated conductivity.

The Millington-Quirk relation with later modifications by Brust, Van Bavel, and Stirck (1968) and Kunze, Uehara, and Graham (1968) may be written as:

$$K(\theta)_i = (1.884)(10)^4 \theta_v^{4/3} n^{-2} \sum_{j=1}^n [(2j + 1 - 2i)h_j^{-2}]$$

$$i = 1, 2, 3, \dots, n \quad (1)$$

where the factor  $(1.884)(10)^4$  is a composite of constants that gives the hydraulic conductivity units of  $\text{cm-min}^{-1}$  and converts the effective pore radius to the pressure potential,  $h$ , in mbars;  $\theta_v$  is the water content as a volume fraction; and  $n$  is the total number of pore intervals.

Mathematical Modeling of Soil-Water Movement

Problems involving the movement of water in unsaturated soils are usually analyzed by two distinct approaches, that is, the quasi-analytical approach and the numerical approach. Watson (1974) stated that "the quasi-analytical approach has been very valuable in presenting a conceptual framework of water movement in unsaturated soils and allowing general statements to be formulated concerning the physics of the phenomena." However, he pointed out that restrictions concerning certain initial and boundary conditions and medium properties eliminates from precise analysis a wide range of problems that are inherent with field conditions. Numerical approaches can be regarded as more suitable for the solution of problems involving many variables and parameters.

The appropriate differential equation for moisture flow in unsaturated soil is generally considered to be of the form:

$$\frac{\partial \theta}{\partial t} = \nabla \cdot (K \nabla h) - \frac{\partial K}{\partial Z} \quad (2)$$

where  $\theta$  is the volumetric water content (dimensionless),  $t$  denotes time (units T),  $\nabla$  is the vector gradient operator,  $K$  is the unsaturated hydraulic conductivity (units L/T),  $h$  is the pressure head (units L), and  $Z$  is the depth with positive values in the downward direction.

Solutions of Eq. (2) for one-dimensional, steady-state flows have been reported by Remson and Fox (1955), Gardner (1958), and Hillel (1971). Solutions are for certain empirical relations between the unsaturated hydraulic conductivity and the soil matric potential. The

lower boundary is, in general, a water table and the upper boundary condition is the flux at the soil surface.

Mathematical modeling of infiltration is reviewed by Philip (1969). Equation (2) can be linearized for steady-state infiltration and isotropic soil when the unsaturated hydraulic conductivity is of the form:

$$K = K_0 \exp(\alpha h) \quad (3)$$

where  $K_0$  is the saturated hydraulic conductivity (units L/T) and  $\alpha$  is an empirical soil constant (units 1/L). Use of Eq. (3) and defining a matric flux potential,  $\phi$ , given by

$$\phi = \int_{-\infty}^h K(h) dh = \frac{K(h)}{\alpha} \quad (4)$$

transforms Eq. (2) into a linear differential equation

$$\nabla^2 \phi = \alpha \frac{\partial \phi}{\partial z} \quad (5)$$

where  $\nabla^2$  is the Laplacian operator.

Philip (1968) solved Eq. (5) for point sources and spherical cavities in an "infinite medium." A generalization of the relationship developed by Philip is reported by Raats (1972) where a description of infiltration from buried point and line sources is discussed for a specified depth.

Gilley and Allred (1972) combined the one-dimensional solution for plane sinks with the two-dimensional solution for line sources to obtain a model for plants removing soil moisture with a subsurface irrigation system. They used the resulting model to estimate the soil-moisture extraction patterns for different values of the soil parameter  $\alpha$ , lateral depth, crop root zone depth, and lateral spacing. A soil-moisture extraction pattern of 40 percent by the crop in the upper 25 percent of the root zone was used to develop design curves relating lateral depth to lateral spacing for different soil types.

Warrick (1974a) extended the steady linearized solution as analyzed by Philip (1968, 1969, 1971), Wooding (1968), and Raats (1970, 1971, 1972) to time-dependent cases for point sources. Included in the analysis were the advance of a wetting front, variation in soil-moisture content resulting from irrigation, and the matric flux potential field for point sources. Lomen and Warrick (1974) investigated time-dependent linearized infiltration from single and parallel surface line sources. Results were considered relevant for high-frequency irrigation, as in a trickle irrigation system, where the soil-moisture content at any particular point varies over a relatively small range.

For a one-dimensional problem and introducing a "sink" term,  $S(Z)$  (units  $1/T$ ), Eq. (5) can be written as:

$$\frac{d^2\phi}{dz^2} - \alpha \frac{d\phi}{dz} - S(Z) = 0 \quad (6)$$

Solution of Eq. (6) for a semi-infinite flow medium and a finite-depth medium overlying a shallow water table was recently proposed by Warrick (1974b). The surface boundary condition was taken as a steady flux and  $S(Z)$  was an arbitrary plant-water withdrawal function. Solutions for exponential and constant sink functions were included.

During the past decade, soil physicists have developed numerous theoretical models for soil-water flow. However, few experiments have been conducted to compare predicted values of soil-water potentials with measured values. Exceptions include Bresler et al. (1971), who compared experimental data for vertical and horizontal water content distribution in the soil profile with predicted values calculated for transient infiltration from a trickle source, as developed in Brandt et al. (1971); and Nimah and Hanks (1973a, 1973b), who developed a mathematical model and numerical solution to predict water content profiles, evapotranspiration, water flow from or to the water table, root extraction, and root water potential under transient field conditions and compared their theoretical results with field measurements. More recently, Thomas et al. (1976) compared capillary potentials measured from laboratory experiments with analytical solutions for steady infiltration from buried line sources. They observed that, in most regions of the soil mass, the calculated capillary potentials were within 25 percent of the measured values. Better agreement between predicted and measured potentials occurred in the soil above the laterals where only a 10 percent discrepancy was observed. However, below the laterals, the calculated capillary potentials were approximately twice the measured values. They explained that

the poor agreement between measured and calculated potentials below the laterals could be caused by: (1) a tendency of the soil to settle, with consequent increase in density with depth and the formation of voids directly below the laterals; (2) the exponential approximation of the hydraulic conductivity and capillary potential relationship; and (3) the lower boundary conditions of the experiment which were not well simulated by the mathematical solution. Criteria for selecting lateral depth and spacing to attain a given capillary potential between laterals were given.

## CHAPTER 3

### EQUIPMENT AND PROCEDURE

#### Equipment and Experimental Setup

Lettuce (*Lactuca sativa* L.) was raised in a greenhouse on the University of Arizona campus at Tucson during the Fall and Winter season 1976-1977.

Four soil bins each 45 cm deep, 55 cm long, and 30.5 cm wide were used to study tension irrigation systems. Four porous ceramic tubes 30.5 cm (12 inches) long and 2.5 cm (1 inch) outside diameter were placed transversely 20 cm deep inside each bin to simulate a plane source. The ceramic tubes were fitted with plastic caps at both ends. A 0.63 cm (0.25 inch) outside diameter copper tube was fastened to the center of the inlet caps to connect to a water supply. A 0.47 cm (0.19 inch) outside diameter copper tube was fastened to the outlet caps, offset near the inside wall of the ceramic tube. The outlet copper tubes were connected to clamped hoses which allowed for periodic removal of air from the system. The ceramic tubes had a wall thickness of 0.31 cm (0.13 inch) and a bubbling pressure of 1 atmosphere.

The flow rate of the ceramic tubes was measured when new and after three months in a soil bin. The relationship between flux and the hydraulic head difference for which the flow was measured is shown in Figure 1. The used ceramic tube was 34 percent less flux than a new one.

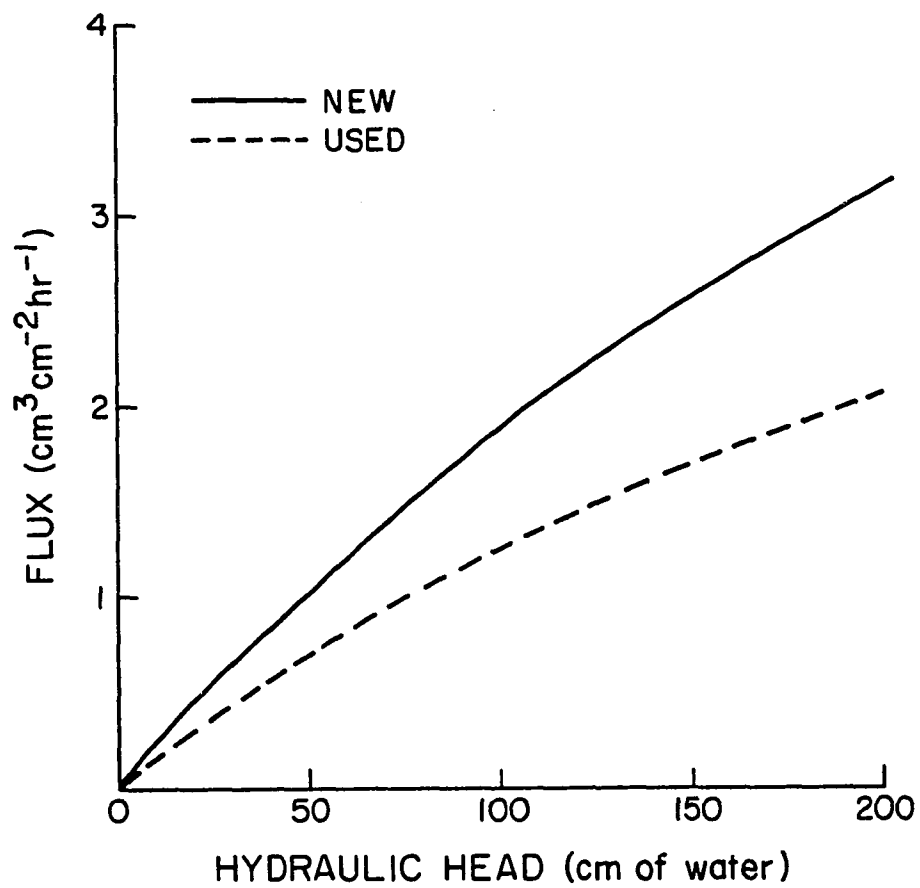


Figure 1. Flux versus Hydraulic Head Relationship for the Ceramic Tubes.

The reasons for the decrease are not known. Distilled water was used so there should have been few particles in the water to cause plugging.

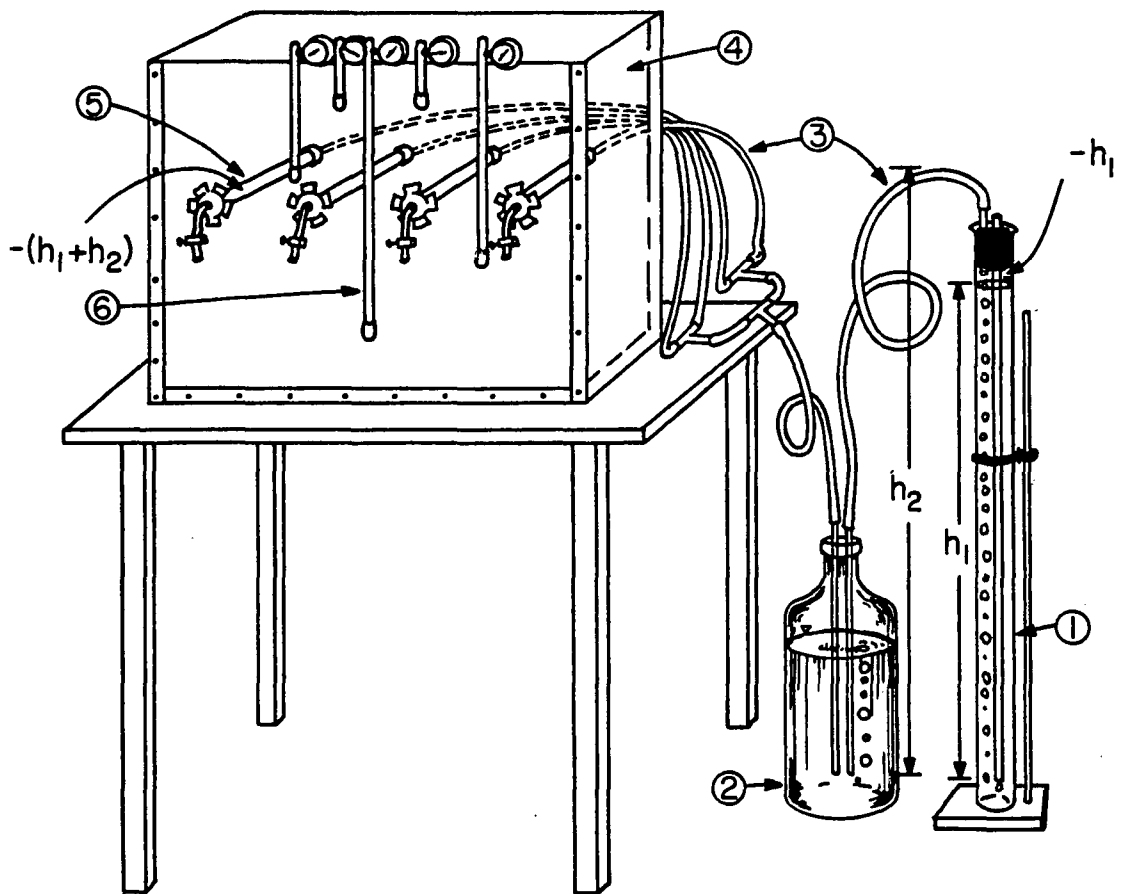
The constant, negative head water delivery system was composed of: (1) calibrated Mariotte bottle; (2) constant head regulator; and (3) plastic tubing and connections. Tensiometers were placed at 8, 18, 29, and 39 cm depths with respect to the soil surface (Figure 2). A hygrothermograph was placed near the soil bins to record air temperature and relative humidity.

### Procedure

#### Soil Preparation and Packing

The soil material used in this study is a Pima clay loam obtained from the University of Arizona experimental farm at Marana. This soil was described and characterized in detail by Pereira (1971). The current taxonomic classification is fine-silty, mixed, thermic family of Typic Torrifluvents, according to the new comprehensive soil classification system (Soil Survey Staff, 1975). The specific particle size analysis for the sample used in this research showed 38 percent clay, 40 percent silt, and 22 percent sand. The air-dried soil was sieved to pass a No. 5 screen (3.96 mm). Superphosphate was mixed with the soil before filling the bins to provide 140 ppm of  $P_2O_5$ .

The soil was packed in the bins by consecutive 5 cm layers. Each layer was carefully mixed with the preceding layer to provide a homogeneous medium. About 90 kg of soil was required to fill each bin within 2 cm of the top. The resulting bulk density was  $1.26 \text{ gm/cm}^3$ .



- |                              |                |
|------------------------------|----------------|
| ① Constant head regulator    | ⑤ Ceramic tube |
| ② Calibrated Mariotte bottle | ⑥ Tensiometer  |
| ③ Plastic hose               |                |
| ④ Soil bin                   |                |

Figure 2. Experimental Setup.

One soil bin was used for the Fall experiment and three for the Winter experiment. The soil bins used in the Winter study were provided with a 5 mm sand layer uniformly distributed on the entire soil surface to prevent crust and crack formation.

#### Lettuce Planting, Thinning, and Nitrogen Application

A pre-planting surface irrigation was applied by flooding the soil surface with a volume of water equivalent to two pore volumes of the soil. The objectives of this initial irrigation were to provide leaching of salts from the soil profile and moisture for germination.

Lettuce seeds were placed approximately 3.8 cm in two rows spaced 27.5 cm apart and transversely located in each bin. Lettuce plants were thinned to one plant per row two weeks after germination. Two applications of 20 ppm of nitrogen (4 gm of urea per soil bin) with the irrigation water were made 15 and 55 days after germination, respectively.

#### Treatments

The soil matric potentials for Fall and Winter experiments were maintained as follows and measured by direct readings of the tensiometers placed at 18 cm depth, i.e., at the plane source level.

1. Fall experiment: -15 to -20 centibars (cbars) soil matric potential during the first 40 days of growing period followed by -30 to -35 cbars until harvest.

2. Winter experiment:

- a. -10 to -15 cbars soil matric potential during the growing season.
- b. -10 to -15 cbars during the first 40 days of growing and -20 to -25 cbars up to harvest.
- c. -10 to -15 cbars during the first 40 days of growing and -30 to -35 cbars up to harvest.

Intake Control and Measurements

In a tension irrigation system, the soil water is continuously connected to the water delivery system through the porous ceramic tubes. The water flow is a function of the negative head and the soil-water potential, resulting from evaporation and transpiration losses. As water is removed, soil-water potential decreases and the water flows from the porous ceramic tubes to the soil medium in response to the hydraulic gradient. The desired tension inside the ceramic tubes was maintained by changing  $h_1$  and  $h_2$  of the pressure regulator apparatus (Figure 2). The gage pressure inside the column, expressed in centimeters of water, is  $-(h_1 + h_2)$ .

Soil matric potentials were recorded daily at about 8:30 a.m. through direct readings from the tensiometers. The consumptive use of water by lettuce was measured directly from the calibrated Mariotte bottle in  $\text{cm}^3$ , also daily at about 8:30. Distilled water was used in all steps of the experiment.

## CHAPTER 4

### RESULTS AND DISCUSSION

Measured values of evapotranspiration, soil matric potentials, and lettuce yield using the tension irrigation systems in the greenhouse are presented. Results are given and discussed for Fall and Winter plantings.

#### Evapotranspiration

##### Fall Experiment

The rate of evapotranspiration (Eta) in mm/day for the September-planted lettuce is shown in Figure 3. The Eta values were estimated using

$$\text{Eta} = \frac{(Q - \Delta S)}{A} \quad (7)$$

where Q is the volume of water read directly from the water supply reservoir in  $\text{cm}^3$ , and  $\Delta S$  is an estimate of the change in the water stored in the soil given by

$$\Delta S = LA(\Delta\theta) \quad (8)$$

where  $\Delta\theta = \theta_1 - \theta_2$  is an estimate of the change in volumetric water content for the time period, L is the total depth in cm, and A is the soil bin area in  $\text{cm}^2$ . The volumetric water content was obtained from

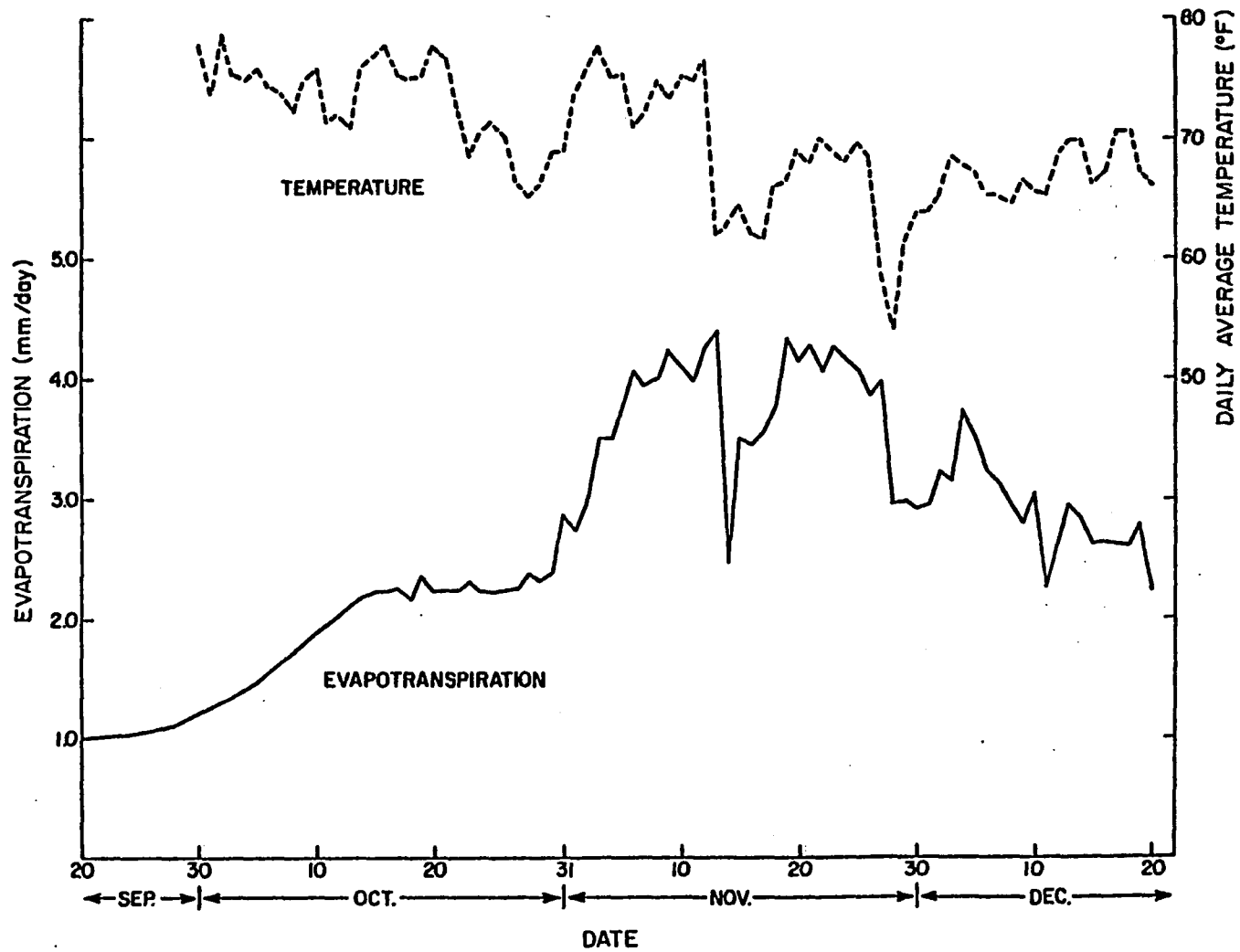


Figure 3. Daily Average Temperature and Evapotranspiration for the Fall Experiment.

tensiometers readings and moisture release data (Figure 10, p. 31). The tensiometers were assumed to give the average soil moisture tension in the surrounding soil layer.

There was a gradual increase in Eta during the first 50 days of growth corresponding to an increase in leaf area and root system development. By November 20, the heads were sufficiently formed that the leaf area remained roughly constant until harvest. The gradual decrease in Eta from November 19 can be attributed to cooler weather and shorter daylight periods.

Average daily temperature and relative humidity values are plotted in Figures 3 and 4. A comparison of the Eta curve with the temperature curve indicates a good correlation of Eta values with air temperature. For example, the drop in Eta values between November 13 and 20 is associated with cold weather for the same period. Similar behavior of the Eta curve is observed in the period of November 27 to December 3. The Eta curve shows daily changes in evapotranspiration and reveals good sensitivity of the tension irrigation system to the consumptive use of water by plants. The highest Eta values were 4.2 mm/day observed between November 9 and 23.

The response in Eta due to daily change in relative humidity was not as evident as that due to change in temperature. However, a comparison of the Eta curve (Figure 3) with the relative humidity curve (Figure 4) indicates that during periods characterized by low relative humidity, as between October 28 and November 9, the Eta values increased.



Figure 4. Daily Average Relative Humidity.

Periods of high relative humidity such as observed from November 13 to 15 had reduced Eta values.

The cumulative evapotranspiration is plotted in Figure 5. Considering a regular growth period of 90 days, the water used is shown to be 240 mm (9.4 inches). This value is near the 8.5 inches estimated under field conditions by Erie et al. (1968) for the same growing season in Mesa, Arizona.

#### Winter Experiment

Daily Eta values for the November-planted lettuce are plotted in Figures 6, 7, and 8 for Treatments I, II, and III, respectively. The Eta values were estimated according to the procedure used for the Fall experiment. An increase in Eta with leaf area was observed during the first 60 days of growth. The sharp rise in Eta between January 10 to 17 was in response to leaf area changes, decreasing relative humidity, and increasing temperature, as shown in Figures 4, 6, 7, and 8 for the period.

During the first 45 days of growth, the three treatments were maintained at the same soil-water potential (-10 to -15 cbars) and Eta curves of Treatments I, II, and III are nearly the same. As the soil-water potentials were changed, a tendency of increasing Eta values with increasing water potentials was observed. This became more evident in the late period of growth when Treatment I reached Eta values as high as 7.0 mm/day compared with 4.4 mm/day for Treatment III. Treatment II shows intermediate Eta values.

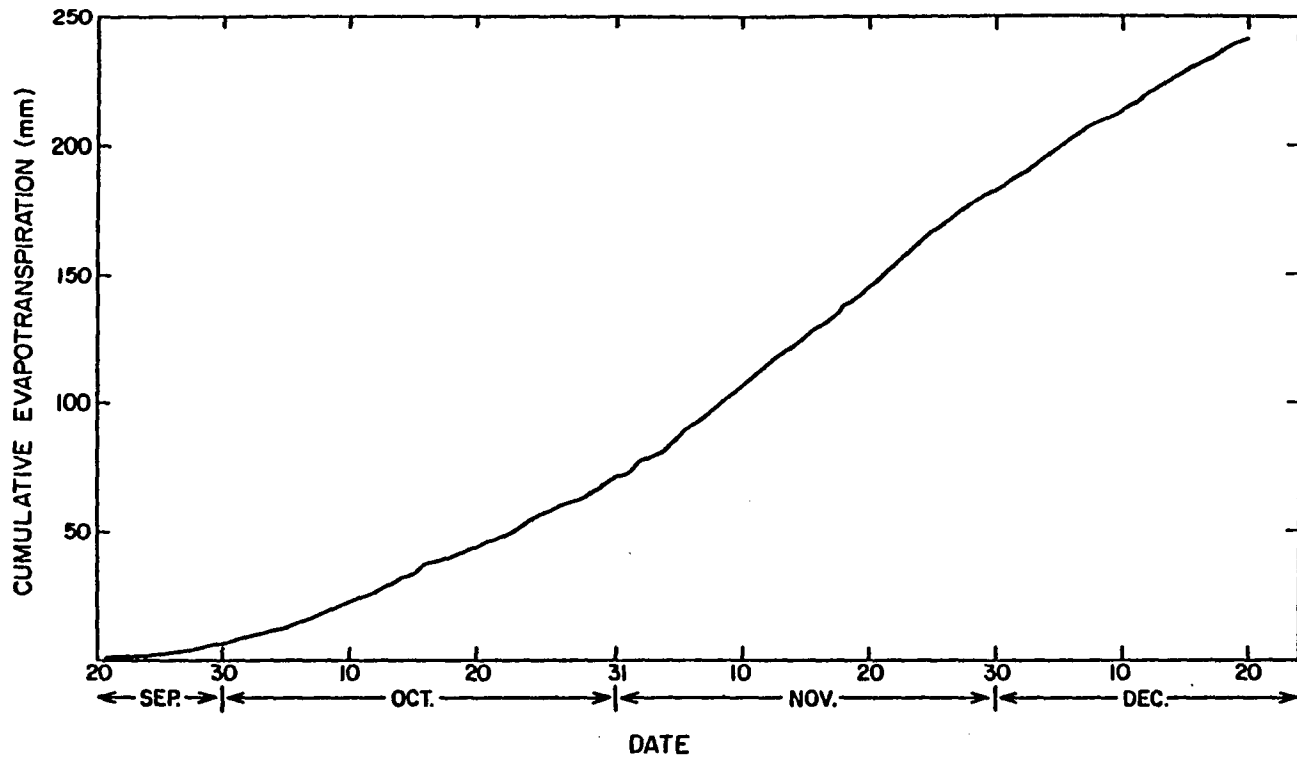


Figure 5. Cumulative Evapotranspiration for the Fall Experiment.

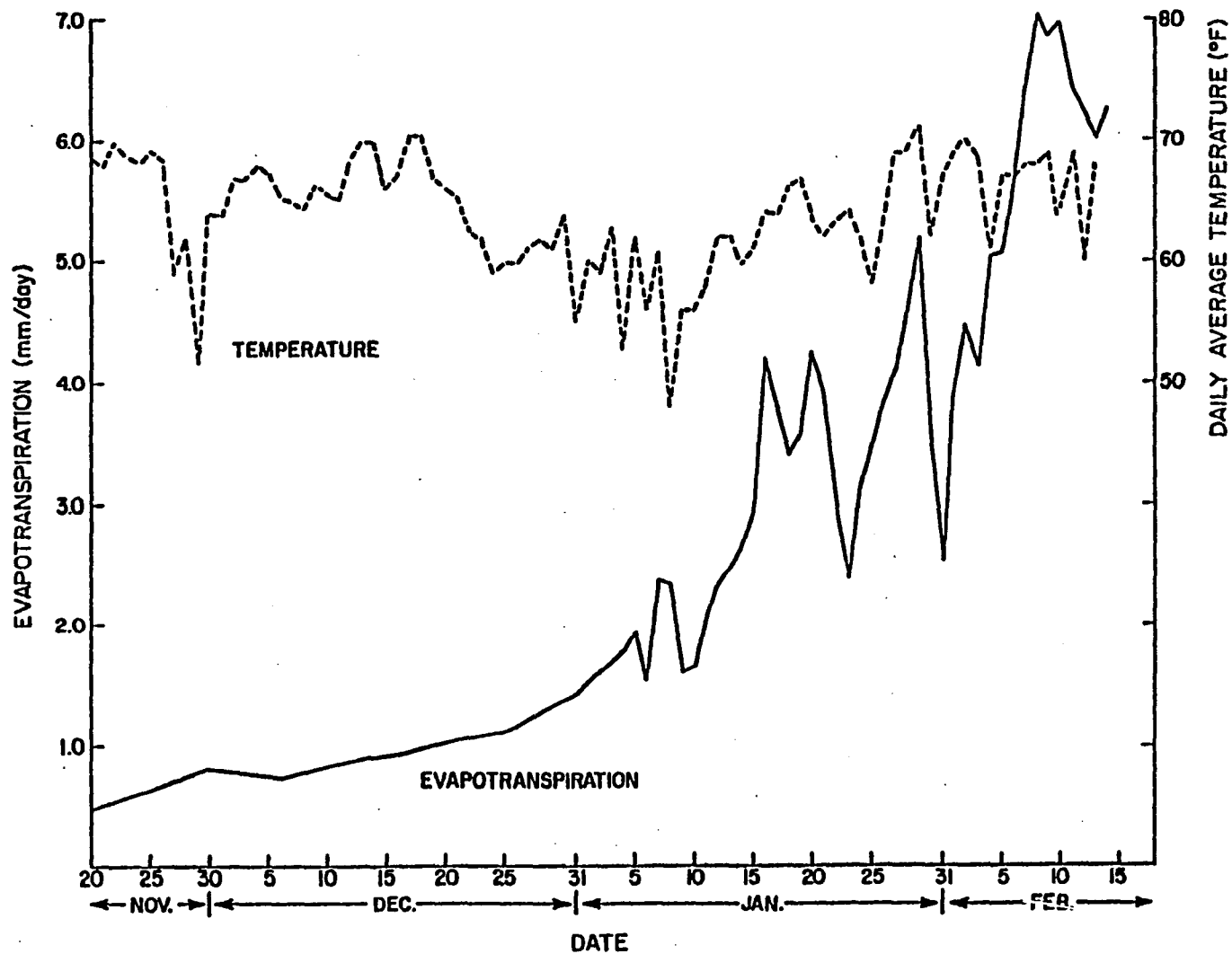


Figure 6. Daily Average Temperature and Evapotranspiration Rate for the Winter Experiment -- Treatment I.

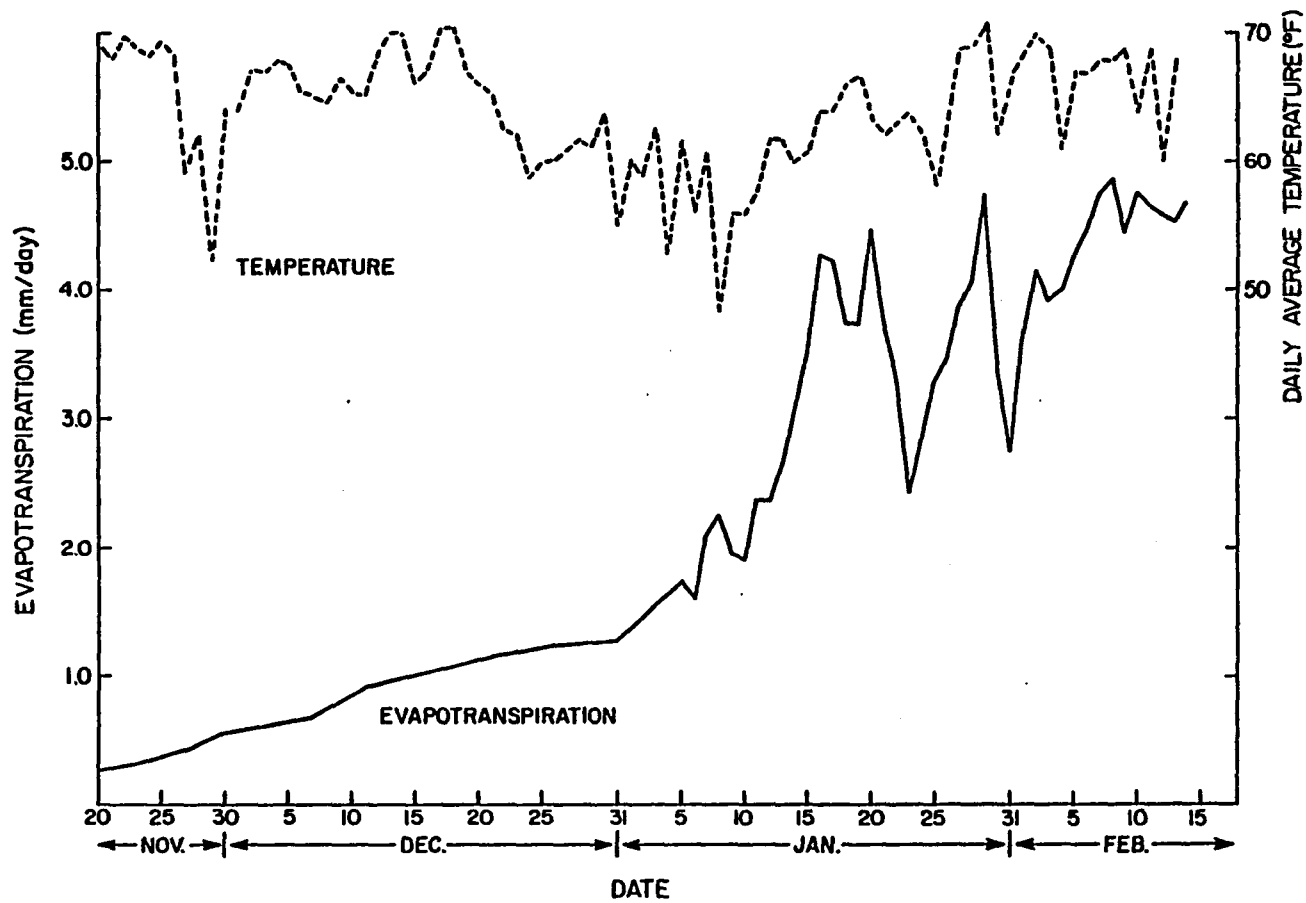


Figure 7. Daily Average Temperature and Evapotranspiration Rate for the Winter Experiment -- Treatment II.

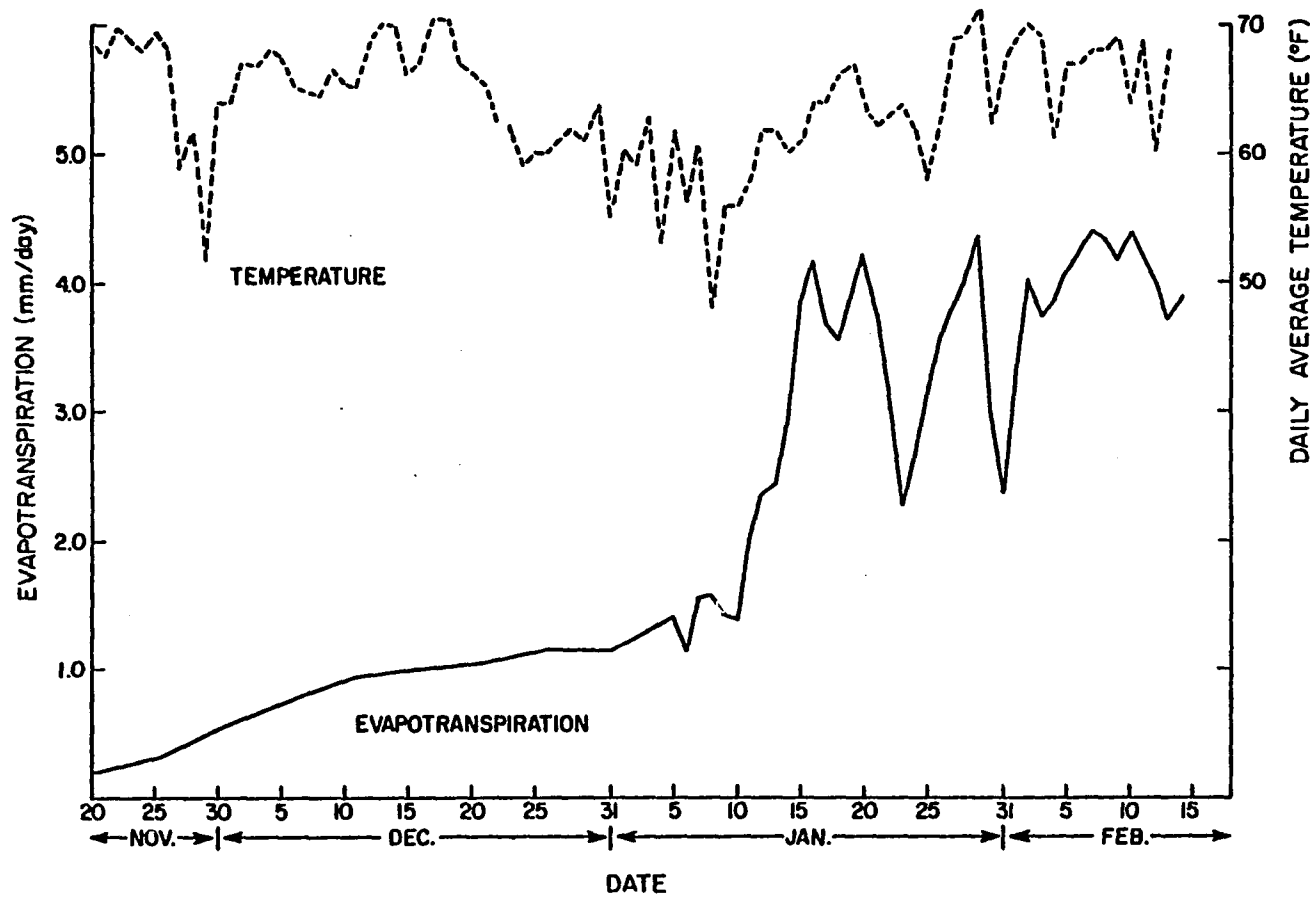


Figure 8. Daily Average Temperature and Evapotranspiration Rate for the Winter Experiment -- Treatment III.

Data of Eta from Treatment I have indicated that, at high soil-water potentials, the consumptive use of water by lettuce was largely determined by atmospheric conditions. However, as soil-water potential decreases, the supply of water to the roots may become a limiting factor and cause a decrease in the rate of transpiration by the leaves on hot and dry days. This can be assumed as one of the main reasons why peak Eta values for Treatments II and III were lower than Treatment I. The peak Eta values of Treatment III from January 15 up to harvest are nearly constant. On the other hand, the peak values of Eta from Treatment I increased during the same period. This is in agreement with increasing temperature and decreasing relative humidity during the time period. The peak Eta values of Treatment II increased after January 15, but remained much lower than Treatment I and slightly higher than Treatment III. This indicates soil moisture tension affects Eta as the highest Eta values correspond to lowest soil moisture tensions and lowest Eta to the highest soil moisture tensions.

The cumulative Eta values of Treatments I, II, and III are plotted in Figure 9. The totals of water used for an 85-day growing period were 206.2 mm (8.1 inches), 187.6 mm (7.4 inches), and 173.9 mm (6.8 inches) for Treatments I, II, and III, respectively.

#### Hydraulic Conductivity of Soil

Values of  $K(\theta)$  were estimated using the moisture release data (Figure 10) and the Millington-Quirk relation (Eq. 1), as used by Jackson et al. (1965), with a matching factor of  $3.6 (10)^4$  in order to give a saturated conductivity of 2.75 cm/hr. The unsaturated hydraulic

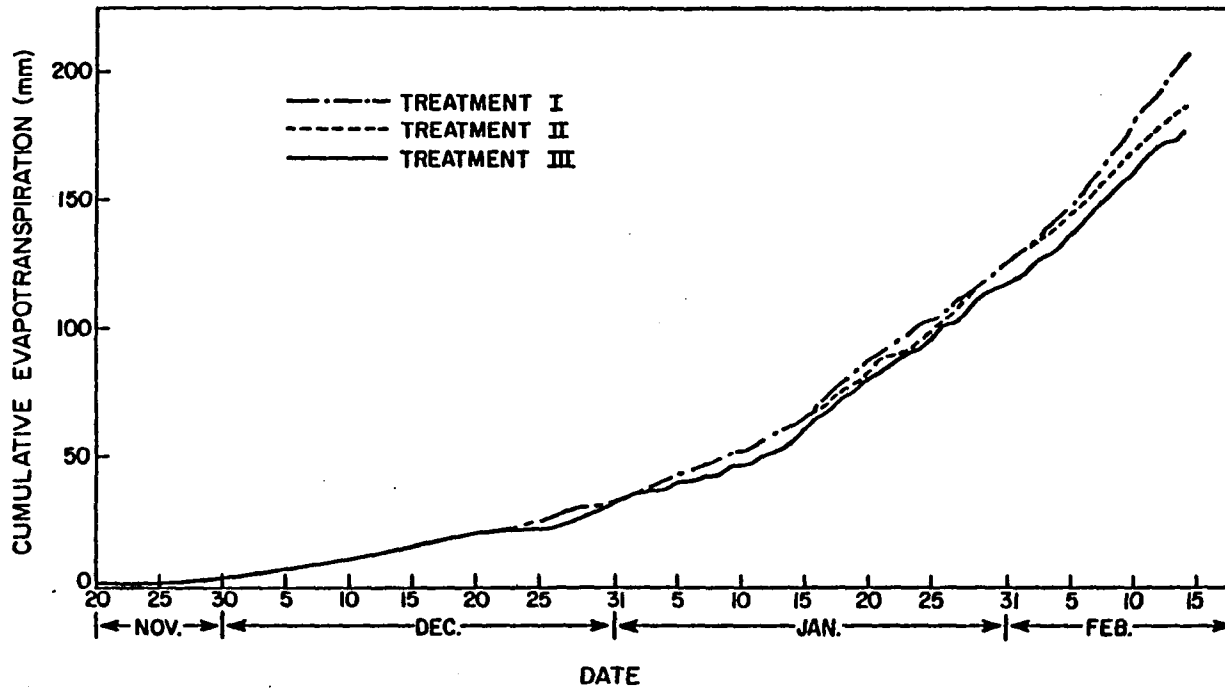


Figure 9. Cumulative Evapotranspiration for the Winter Experiment.

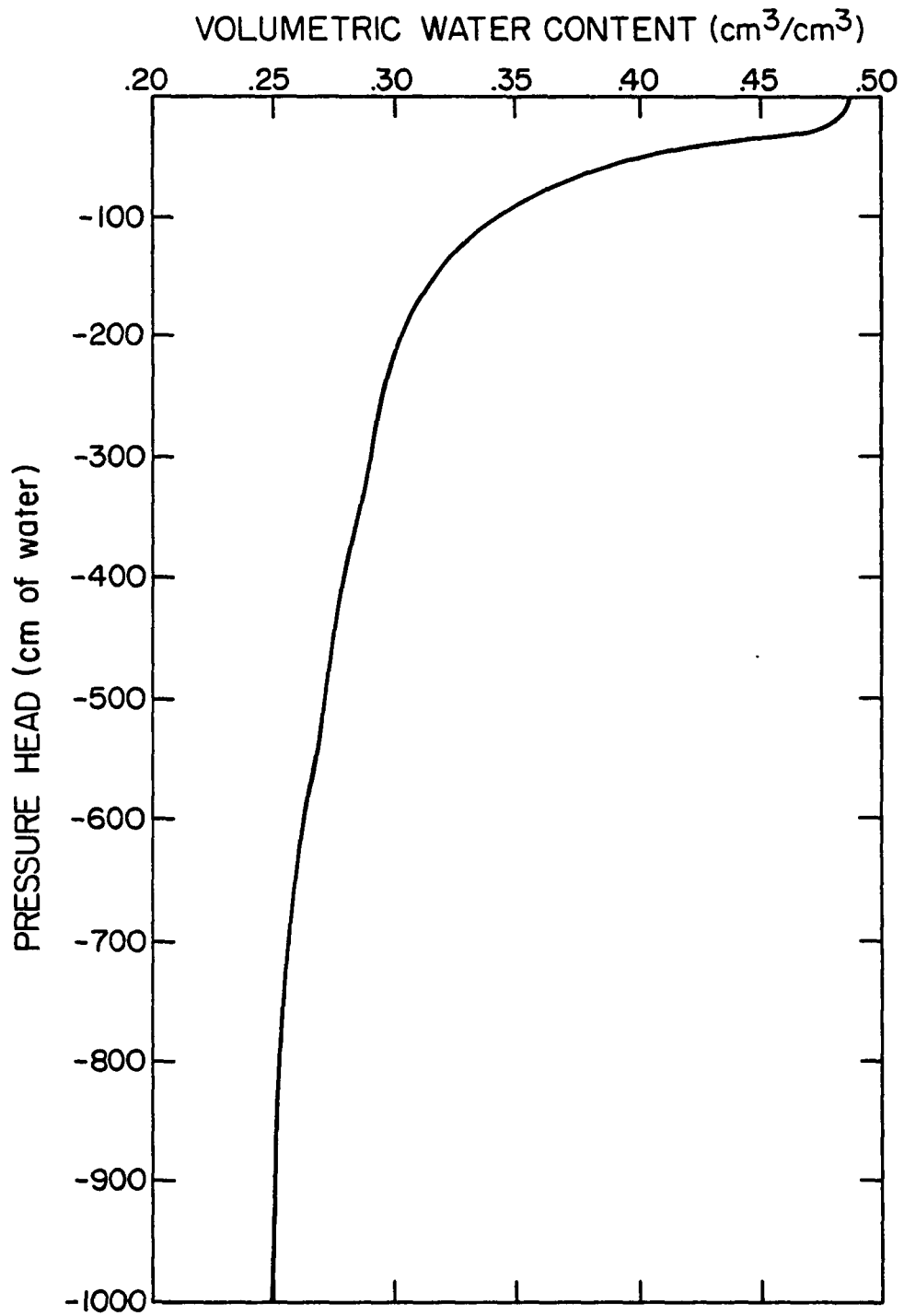


Figure 10. Moisture Characteristic Curve for Pima Clay Loam.

conductivity values of the soil as a function of the volumetric water content,  $\theta$ , are plotted in Figure 11. The capillary conductivity and pressure head relationship values plotted in Figure 12 were determined using data from the  $K$  versus  $\theta$  (Figure 11) and moisture release (Figure 10).

#### Measured Soil Matric Potentials

The soil matric potential values for the Fall and Winter experiments were recorded directly from readings of the tensiometers and are presented in the Appendix. For both Fall and Winter experiments, a nearly uniform soil matric potential with depth was maintained by the tension irrigation system during the first 40 days of growth. Later adjustments of the soil-water potentials to meet pre-established treatments as well as the increase of the evapotranspiration demand caused a hydraulic gradient formation upward and downward from the plane source. A nearly steady-state condition was observed from November 16 to December 6 and January 15 to February 3 for the Fall and Winter experiments, respectively. The soil matric potential average values in centimeters of water for the above periods are presented in Table 1.

#### Flow Resistance and Change in the Negative Head

The flow resistance from the ceramic tubes to the soil increases with decreasing soil matric potential. At the end of the growing season, the water pressures inside the ceramic tubes were -25, -21, and -15 cm of water (see Appendix, Tables A2, A3, and A4). The corresponding soil matric potentials measured near the ceramic tubes were -151, -237, and

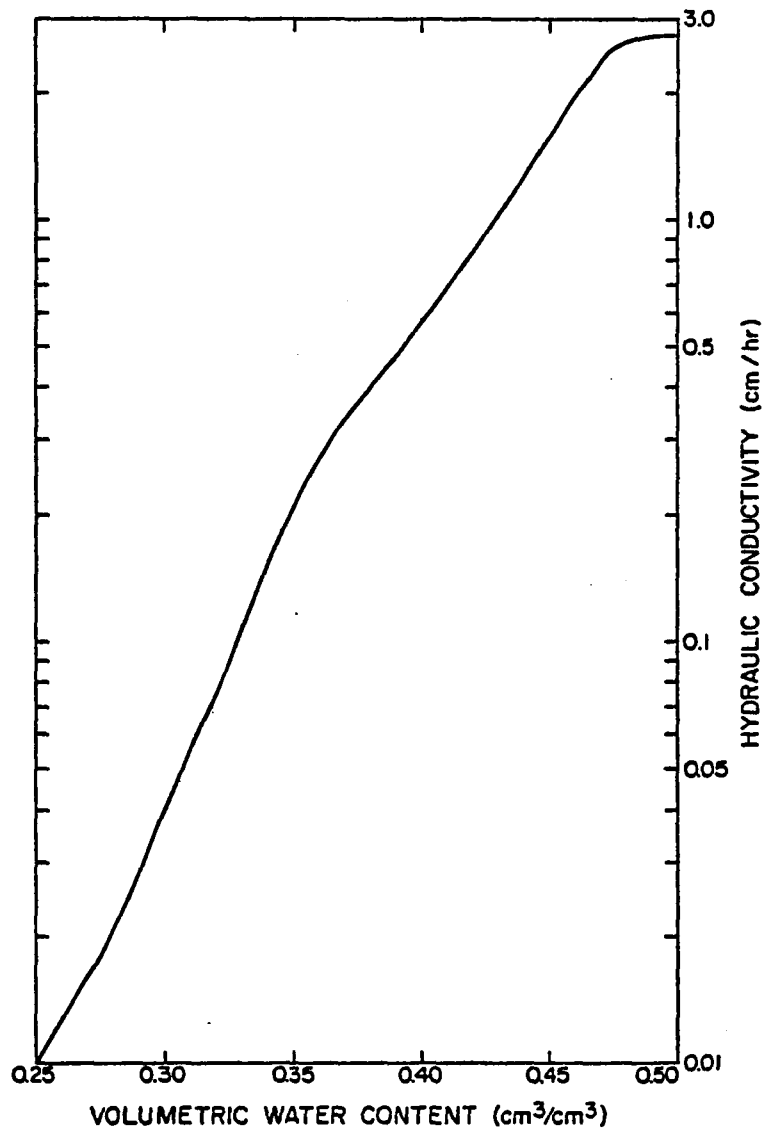


Figure 11. Hydraulic Conductivity and Volumetric Water Content Relationship for Pima Clay Loam.

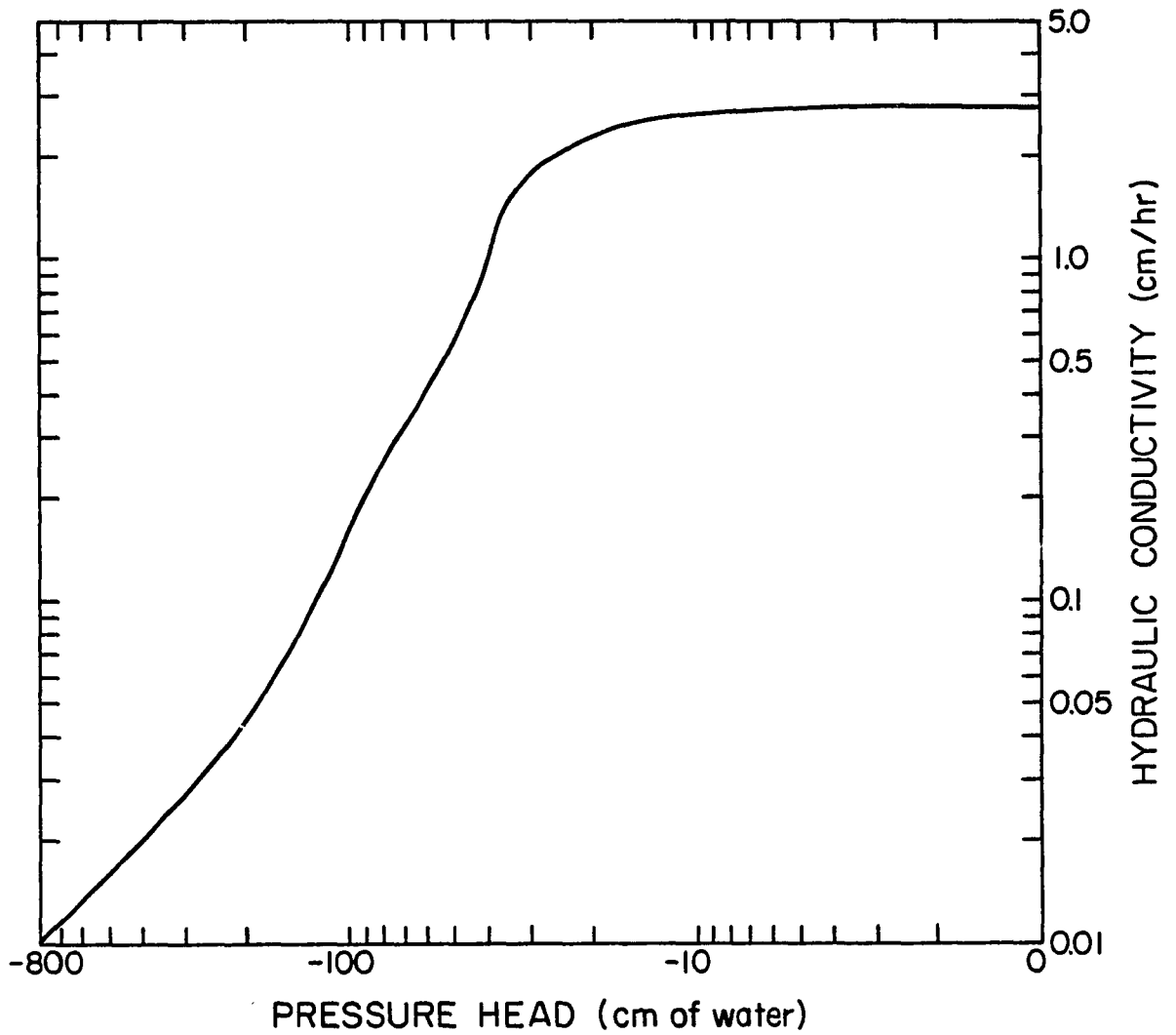


Figure 12. Hydraulic Conductivity and Pressure Head Relationship for Pima Clay Loam.

Table 1. Twenty-Day Average of Soil Matric Potentials for the Fall and Winter Experiments.

Tensiometer Depth (cm)	Soil Matric Potentials (-cm of Water)			
	Fall	Winter		
		I	II	III
8	462	182	266	381
18	341	151	237	341
29	551	209	350	513
39	655	225	427	690

-341 cm of water. Consequently, the effective change in potentials between the ceramic tube and the soil to maintain the required flow rates (keep the soil matric potential nearly constant) were -126, -216, and -326 cm of water for Treatments I, II, and III, respectively.

The change in potentials between the ceramic tube and the soil is expected to vary with the unsaturated hydraulic conductivity of the soil, permeability of the porous ceramic tubes, flow rate required, root density, and the contact area between the surface of the porous material and soil. The unsaturated hydraulic conductivity is one of the major factors that affects this change in potential. For example, from Figure 12, the hydraulic conductivity decreases from  $6.6 (10)^{-2}$  to  $2.3 (10)^{-2}$  cm/hr when h values change from -151 cm (Treatment I) to -341 cm (Treatment III). Also, void formation between the ceramic tube and the soil as soil matric potential decreases can greatly increase flow resistance due to the reduction in the effective flow area.

The periodic adjustment of the negative head (see Appendix, Tables A1, A2, A3, and A4) was necessary because of the reduced flow through the ceramic tubes (Figure 1) and increasing evapotranspiration demand.

#### Lettuce Yield

The lettuce yield for the Fall and Winter experiments is shown in Table 2. In both cases, yield is expressed as fresh weight of head lettuce after removal of external leaves. Also, the data represent an average of two plants per soil bin which is equivalent to one plant per  $839 \text{ cm}^2$  or 48,250 plants per acre.

Table 2. Lettuce Yield for Fall and Winter Experiments.

Growing Season	Lettuce Yield (gm/plant)
Fall	940
Winter:	
Treatment I	924
Treatment II	1,060
Treatment III	1,121

The Winter experiment showed a tendency of increasing lettuce fresh weight with decreasing soil water potential. The reasons for this are not certain. However, from Figure 10, the soil porosity is about 49% and the volumetric water content at  $h = -120$  cm of water is 34%. Consequently, limiting soil aeration (15% air space) seems to be an important factor responsible for the low lettuce fresh weight of Treatment I. In addition, the high soil-water potential was maintained nearly uniform with depth by the tension irrigation system. The more effective hydraulic gradient in Treatments II and III resulted in a zone of higher water potential near the plane source (easy uptake) and two zones of lower water potential (high aeration) upward and downward away from the plane source. Consequently, a better soil-water-plant-atmosphere relationship was accomplished.

## CHAPTER 5

### COMPARISONS OF CALCULATED AND MEASURED SOIL MATRIC POTENTIALS

The development of a one-dimensional soil-moisture model and comparison between the predicted and observed values of the soil matric potential are now presented. The results are discussed for the Fall and Winter experiments.

#### One-Dimensional Soil-Moisture Model

The solution of Eq. (6) for a semi-infinite medium and a constant surface flux,  $v_0$  (units L/T), is (Warrick, 1974b):

$$\phi = \frac{v_0}{\alpha} - \exp(\alpha Z) \int_Z^{\infty} \exp(-\alpha Z') \int_0^{Z'} S(\xi) d\xi dZ' \quad (9)$$

where  $S(Z)$  is the volume of water removed per unit volume of soil per unit time, and  $Z'$  and  $\xi$  are dummy integration variables. For  $S(Z) = a$  (units 1/T) in the root zone ( $0 < Z < L$ ) and 0 elsewhere ( $Z > L$ ), Eq. (9) becomes (Warrick, 1974b, Table 1):

$$\phi_s = -\frac{a}{\alpha^2} (\alpha Z + 1) + \frac{a}{\alpha^2} \exp[\alpha(Z - L)], \quad 0 < Z < L \quad (10)$$

and

$$\phi_s = -\frac{aL}{\alpha}, \quad Z > L \quad (11)$$

where  $v_0$  is taken as zero,  $L$  is the rooting depth, and the subscript "s" denotes sink.

#### Plane Sink

The appropriate relationship for a plane sink can be found using Eqs. (10) and (11) and the superposition principle. Consider a sink function as Figure 13A, with  $S(Z) = a$  for  $0 < Z < d+\Delta d$  and  $S(Z) = 0$  for  $Z > d+\Delta d$ . The solution,  $\phi_{s,1}(Z)$ , for this uptake is by Eqs. (10) and (11):

$$\phi_{s,1}(Z) = -\frac{a}{\alpha^2} (\alpha Z + 1) + \frac{a}{\alpha^2} \exp [\alpha(Z - d - \Delta d)], \quad 0 < Z < d + \Delta d \quad (12)$$

and

$$\phi_{s,1}(Z) = -\frac{a}{\alpha} (d + \Delta d), \quad Z > d + \Delta d \quad (13)$$

Consider a second function  $S(Z) = a$  for  $0 < Z < d$  and  $S(Z) = 0$  for  $Z > d$  as in Figure 13B. This will correspond to a source in the region 0 to  $d$ . The solution,  $\phi_{s,2}(Z)$  is by Eqs. (10) and (11):

$$\phi_{s,2}(Z) = \frac{a}{\alpha^2} (\alpha Z + 1) - \frac{a}{\alpha^2} \exp [\alpha(Z - d)], \quad 0 < Z < d \quad (14)$$

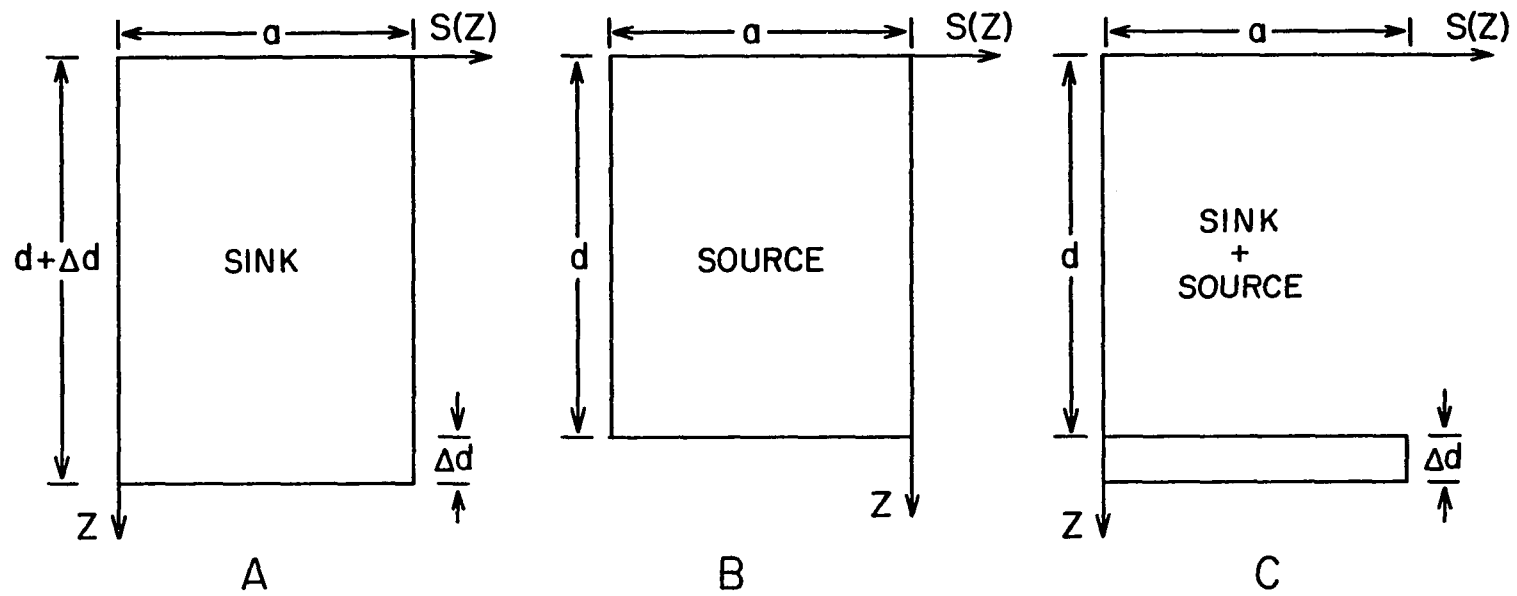


Figure 13. Geometry of the Flow Problem.

and

$$\phi_{s,2}(Z) = \frac{ad}{\alpha}, \quad Z > d \quad (15)$$

If we add Eqs. (12) and (14) together, the result is

$$\phi_s = \frac{a}{\alpha} \{ \exp[\alpha(Z - d - \Delta d)] - \exp[\alpha(Z - d)] \} \quad (16)$$

This corresponds to the uptake pattern shown in Figure 13C, i.e., no uptake for  $Z < d$  or  $Z > d + \Delta d$ , but with  $S(Z) = a$  for  $d < Z < d + \Delta d$ . The net uptake,  $u$  (units L/T), is given by  $u = a\Delta d$ . The solution for a plane sink is evaluated in the limit as  $\Delta d \rightarrow 0$ , but keeping  $u$  finite:

$$\phi_s = -\frac{u}{\alpha} \exp[\alpha(Z - d)], \quad 0 < Z < d \quad (17)$$

If we add Eqs. (13) and (15), we find as  $\Delta d$  approaches 0 and below the sink

$$\phi_s = -\frac{a\Delta d}{\alpha} = -\frac{u}{\alpha}, \quad Z > d \quad (18)$$

Equations (17) and (18) are in agreement with Eqs. (14) and (15) (plane sink term) in Gilley and Allred (1972).

#### Plane Source

Multiplication of the right side of Eqs. (17) and (18) by (-1) reverses the flux direction, so

$$\phi_{ps} = \frac{u}{\alpha} \exp[\alpha(Z - d)], \quad 0 < Z < d \quad (19)$$

and

$$\phi_{ps} = \frac{u}{\alpha}, \quad Z > d \quad (20)$$

where the subscript "ps" denotes plane source and u becomes the source strength.

#### Infiltration Model

Adding Eqs. (19) with (10) and then (20) with (10) and taking  $u = aL$ :

$$\begin{aligned} \phi(Z) = (\phi_{ps} + \phi_s) &= \frac{aL}{\alpha} \exp [\alpha(Z - d)] - \frac{a}{\alpha^2} (\alpha Z - 1) \\ &+ \frac{a}{\alpha^2} \exp [\alpha(Z - L)] \end{aligned} \quad (21)$$

above a plane source, and

$$\phi(Z) = (\phi_{ps} + \phi_s) = \frac{aL}{\alpha} - \frac{a}{\alpha^2} (\alpha Z - 1) + \frac{a}{\alpha^2} \exp [\alpha(Z - L)] \quad (22)$$

below a plane source.

The solution can be expressed in terms of the pressure head by substituting the above values of  $\phi$  into

$$h = \ln [\alpha\phi/K_0]/\alpha \quad (23)$$

### Numerical Calculations

It is assumed that the buried ceramic tubes are sufficiently close that they can be mathematically represented by a plane source.

#### Fall Experiment

The plane source strength,  $u$ , was  $1.52 (10)^{-2} \text{ cm}^3 \text{ cm}^{-1} \text{ sec}^{-1}$ . This value corresponds to a 20-day average of  $E_t$  between November 17 and December 6 (Appendix, Table A1) and represents a water application (irrigation rate  $u = aL$ ) of  $3.66 \text{ mm day}^{-1}$ . For this irrigation rate and  $L$  equal to 43 cm, the "a" value is  $0.00852 \text{ day}^{-1}$ .

The soil matric potentials were first calculated using Eq. (23) where the functions of  $\phi(Z)$  are given for uniform uptake rate by Eqs. (21) and (22). The value of  $K_0$  used in Eq. (3) was  $1.5 \text{ cm day}^{-1}$ , which is the hydraulic conductivity value for the soil matric potential of -160 cm of water (Figure 12). The saturated conductivity value (66 cm/day), when substituted in Eq. (23), resulted in  $h$  values that did not match with measured values of the soil matric potentials. This is probably caused by the completely unsaturated nature of the soil-moisture flow with the tension irrigation system. The exponential relationship  $K = 1.5 \exp(\alpha h) \text{ cm day}^{-1}$  between the hydraulic conductivity and pressure head for values of  $\alpha$  equal to 0.0117, 0.016, and  $0.023 \text{ cm}^{-1}$  is plotted in Figure 14. Also shown are values of  $K$  estimated from the Millington-Quirk method as in Figure 12, but with a "matching factor" chosen to give  $K_0 = 1.5 \text{ cm/day}$  at  $h = 0$ . The value of  $\alpha$  for the best fit to experimental values of the capillary potential (Table 1) was  $0.0117 \text{ cm}^{-1}$ . The calculated capillary potential distribution as a function of  $Z/L$  is

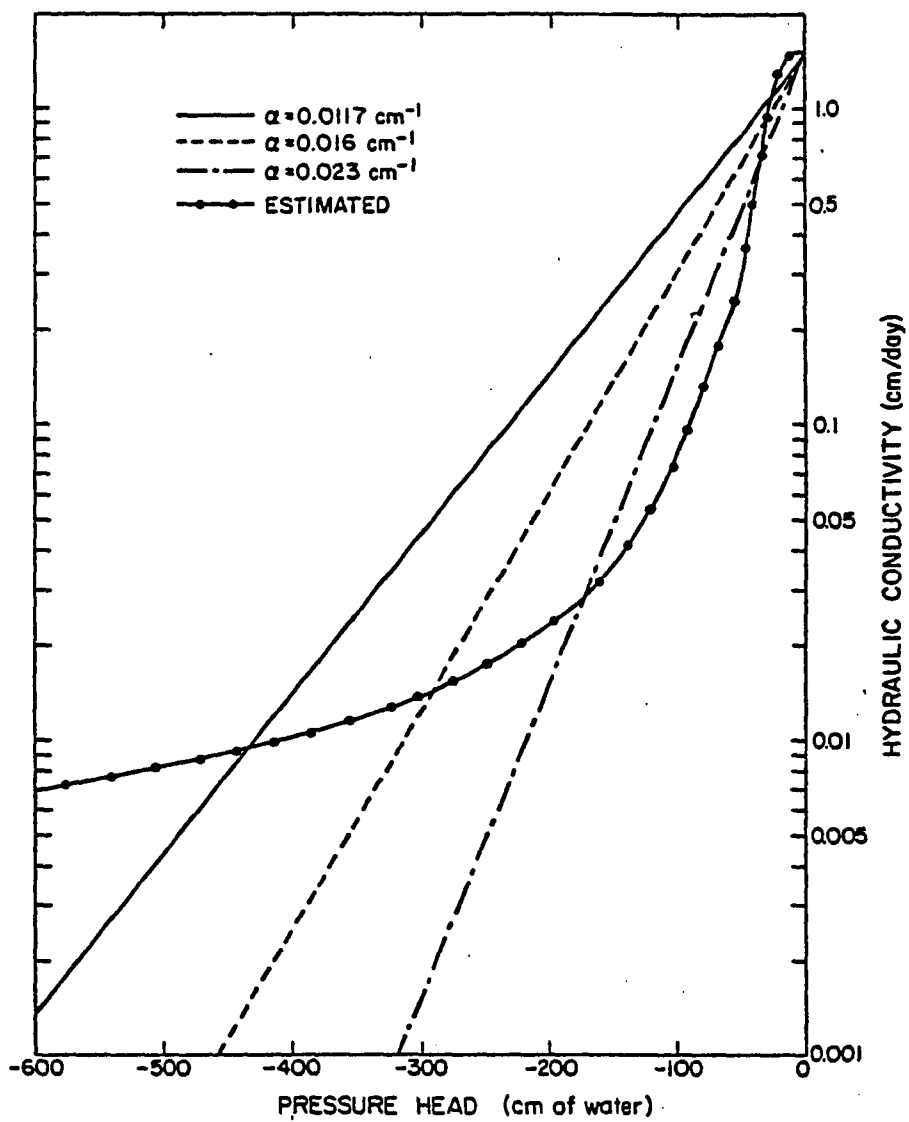


Figure 14. Hydraulic Conductivity and Capillary Potential Relationship for Pima Clay Loam.

plotted (dashed line) in Figure 15. The measured potentials are also plotted for comparison. Calculated values of the pressure heads greatly overestimated the observed values in the region of the soil mass above the plane source.

In order to find a better agreement, a 60 percent water withdrawal pattern by the plants in the top 22 cm of the root zone was then studied with the other 40 percent withdrawal below. This uptake pattern is represented graphically in Figure 16 and it corresponds to

$$u_1 = a_1 L_1 + a_2 L_1 = 0.6 \text{ aL}$$

and

$$u_2 = a_2 (L_2 - L_1) = 0.4 \text{ aL}$$

or

$$a_1 = 0.00301 \text{ day}^{-1}$$

and

$$a_2 = 0.00698 \text{ day}^{-1}$$

The matric flux potential,  $\phi(Z)$ , then became

$$\phi(Z) = \phi_{ps} + \phi_s = \phi_{ps} + (\phi_{s,1} + \phi_{s,2}) \quad (24)$$

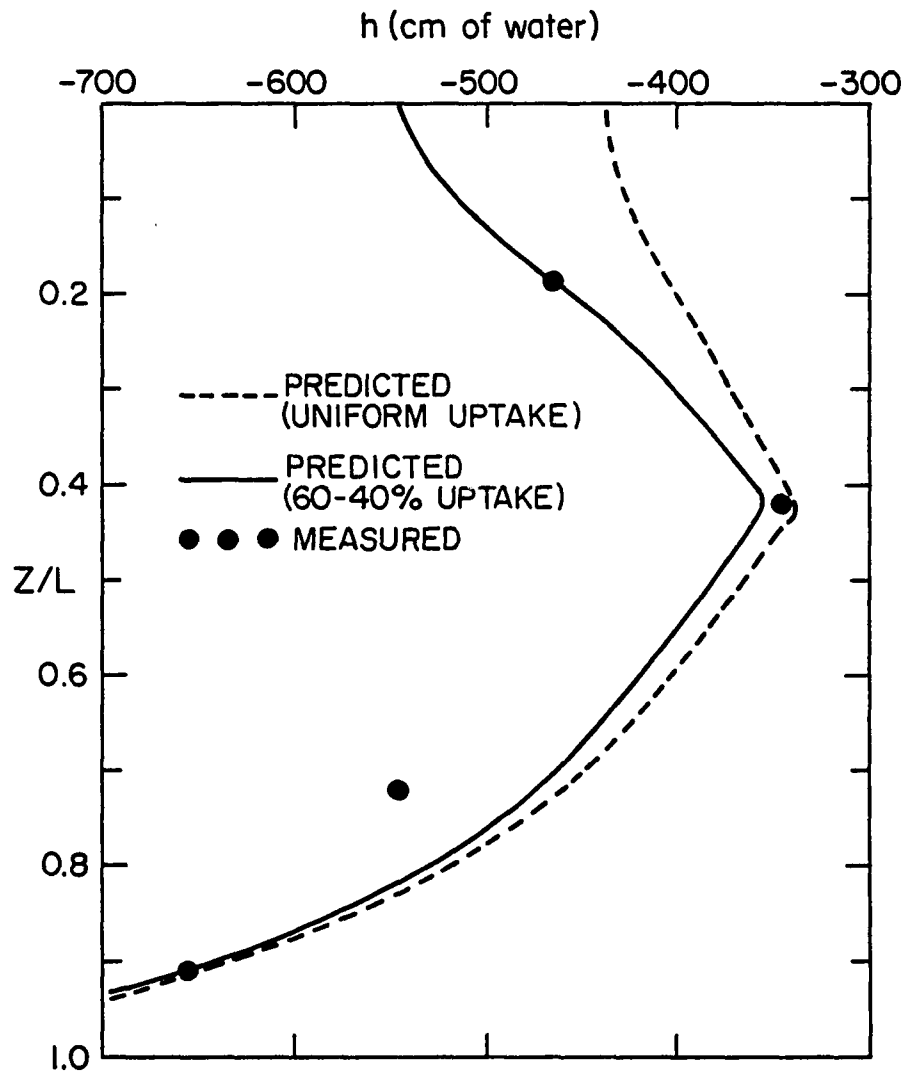


Figure 15. Comparison of the Predicted and Measured Pressure Head for Uniform and Non-Uniform Water Withdrawal Patterns for the Fall Experiment.

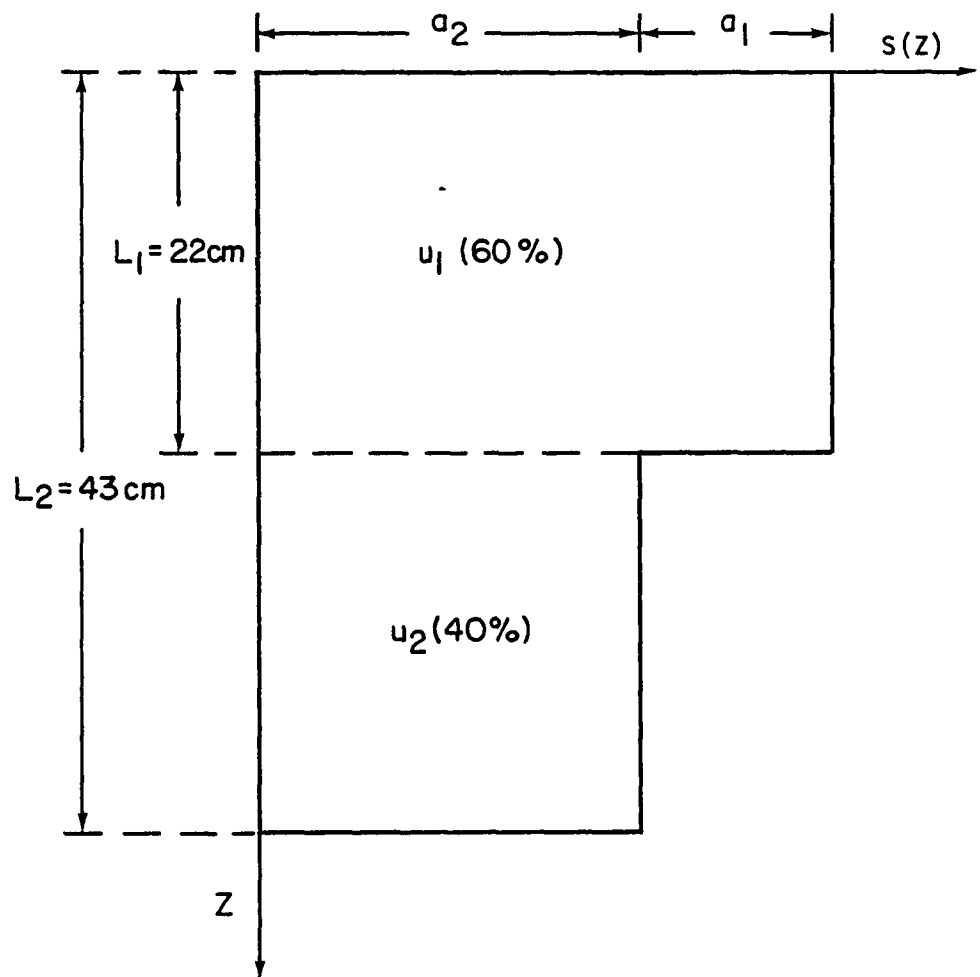


Figure 16. Uptake Pattern.

From Eqs. (8) and (9)

$$\phi_{s,1} = -\frac{a_1}{\alpha^2} (\alpha Z + 1) + \frac{a_1}{\alpha^2} \exp [\alpha(Z - L_1)] , \quad 0 < Z < L_1 \quad (25)$$

$$\phi_{s,1} = -\frac{a_1 L_1}{\alpha} , \quad Z > L_1 \quad (26)$$

$$\phi_{s,2} = -\frac{a_2}{\alpha^2} (\alpha Z + 1) + \frac{a_2}{\alpha^2} \exp [\alpha(Z - L_2)] , \quad 0 < Z < L_2 \quad (27)$$

Substitution of  $\phi(Z)$  from Eq. (24) into Eq. (23) gave the capillary potential distribution (full line) shown in Figure 15.

The surface values of  $h$  are about -437 cm and -546 cm for the uniform and non-uniform uptake rate, respectively. When comparing the measured and calculated capillary potential at  $Z = 8$  cm, it can be observed that the calculated value was within 11 percent of the measured value for the uniform uptake case. Also, at  $Z = 29$  cm, the calculated capillary potentials were within 16 percent of the measured value. These differences between measured and calculated potentials decreased to about 3 percent and 12 percent for  $Z$  equal 8 and 29 cm, respectively, with a 60% water withdrawal pattern in the upper 22 cm of the root zone. At  $Z = 18$  cm (plane source level) and  $Z = 39$  cm, the differences between measured and calculated capillary potential values remained nearly the same for the uniform and non-uniform uptake pattern.

The calculated values for each term of Eq. (24) as a function of  $Z/L$  are in Table 3. Also, the calculated values of  $h$  (-cm of  $H_2O$ ) from Eq. (23) and  $K$  ( $= \alpha\phi$ ) from Eq. (3) are included in Table 3.

#### Winter Experiment

The plane source strengths,  $u$ , were  $1.56 (10)^{-2}$ ,  $1.54 (10)^{-2}$ , and  $1.48 (10)^{-2} \text{ cm}^3 \text{ cm}^{-1} \text{ sec}^{-1}$  for Treatments I, II, and III, respectively. These values correspond to a 20-day average  $E_t$  between January 16 and February 4 (Appendix, Tables A2, A3, and A4) and represent water applications (irrigation rate  $u = aL$ ) of 3.76, 3.70, and 3.55 mm/day. For these irrigation rates and  $L$  equal to 43 cm, the "a" values are 0.00876, 0.00845, and  $0.00861 \text{ day}^{-1}$  for Treatments I, II, and III, respectively.

The soil matric potentials plotted as a function of  $Z/L$  in Figures 17, 18, and 19 were calculated using Eq. (23) where the functions of  $\phi(Z)$  are given in Eqs. (21) and (22). Also, the measured potentials from Table 1 are plotted for comparison. The same exponential relationship between the hydraulic conductivity and pressure head used in the Fall experiment (Figure 14) was applied where the values of  $\alpha$  that correspond to the best fit to observed soil matric potentials were 0.023, 0.016, and  $0.0117 \text{ cm}^{-1}$  for Treatments I, II, and III, respectively.

The agreement between measured and computed soil matric potentials was, in general, good for the three soil-water levels studied. The calculated capillary potentials were within 7 percent of the measured values except for the 29 cm depth of Treatments II and III and the 39 cm depth of Treatment I that was within 13 and 21 percent, respectively.

Table 3. Calculated Matric Flux Potentials, Capillary Potentials, and  $K(=\alpha\phi)$  as a Function of  $Z/L$ .

$z = Z/L$	$\phi_{ps}(Z)$ ( $\text{cm}^2 \text{day}^{-1}$ )	$\phi_{s,1}(Z)$ ( $\text{cm}^2 \text{day}^{-1}$ )	$\phi_{s,2}(Z)$ ( $\text{cm}^2 \text{day}^{-1}$ )	$\phi(Z)$ ( $\text{cm}^2 \text{day}^{-1}$ )	$h$ ( $-\text{cm H}_2\text{O}$ )	$K(=\alpha\phi)$ ( $\text{cm day}^{-1}$ )
.00	25.366	-4.996	-20.152	0.216	545	0.0025
.05	25.967	-5.108	-20.615	0.242	536	0.0028
.12	26.894	-5.259	-21.278	0.357	503	0.0041
.19	27.855	-5.387	-21.899	0.568	463	0.0066
.23	28.514	-5.460	-22.291	0.763	438	0.0089
.30	29.533	-5.549	-22.842	1.141	403	0.0133
.37	30.588	-5.614	-23.350	1.624	373	0.0190
.42	31.312	-5.643	-23.662	2.006	355	0.0234
.51	"	-5.667	-24.225	1.419	385	0.0166
.58	"	"	-24.590	1.054	410	0.0123
.70	"	"	-25.084	0.560	464	0.0065
.81	"	"	-25.429	0.216	545	0.0025
.91	"	"	-25.590	0.054	663	0.0006
.95	"	"	-25.631	0.013	782	0.0002

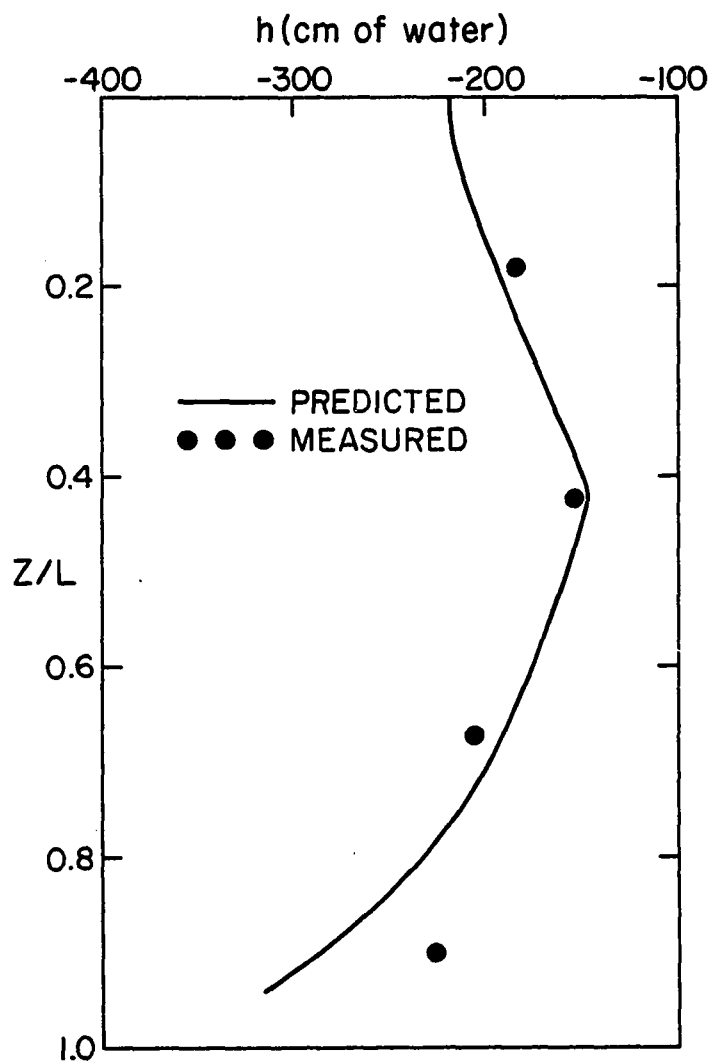


Figure 17. Comparison of the Predicted and Measured Pressure Head for the Winter Experiment -- Treatment I.

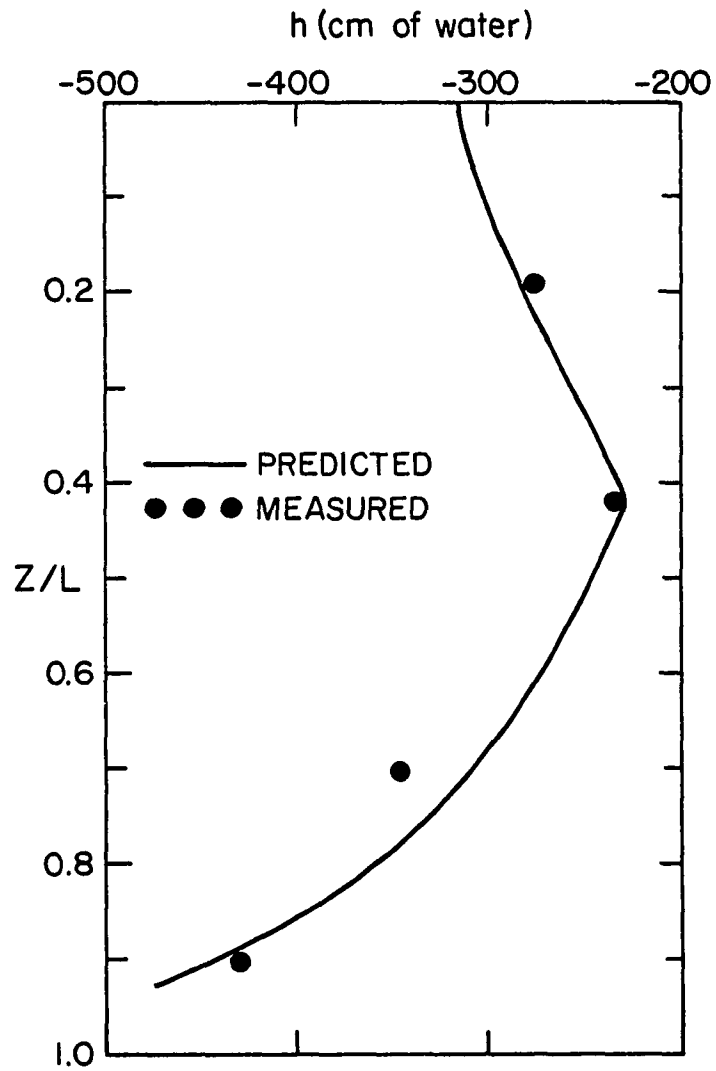


Figure 18. Comparison of the Predicted and Measured Pressure Head for the Winter Experiment -- Treatment II.

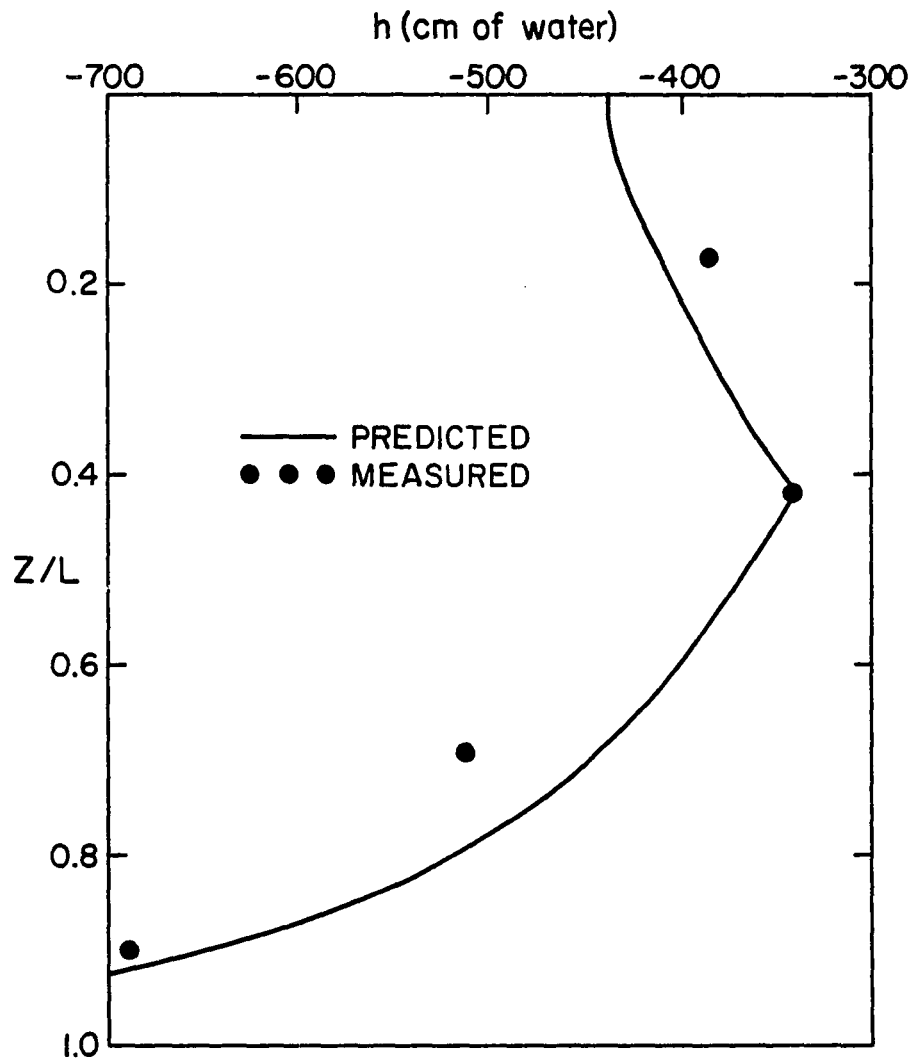


Figure 19. Comparison of the Predicted and Measured Pressure Head for the Winter Experiment -- Treatment III.

The poor agreement between calculated and measured values of the capillary potentials at 29 cm depth for the drier treatments could be caused by a higher plant root density in the region just below the plane source. This seems to be a reasonable assumption because, with a subsurface irrigation system, there is a tendency for the plant rooting system to be deeper because of drier soil near the soil surface. On the other hand, the discrepancy observed between calculated and predicted capillary potentials at the 39 cm depth of Treatment I can be associated with the lower boundary condition, i.e., the lower boundary condition for the wettest soil water regime was not simulated accurately by the mathematical solution.

The control of the capillary potentials away from the source by the tension irrigation system was better for the wetter treatments than for the drier ones. This is because of the rapid decrease of the unsaturated hydraulic conductivity of the soil with  $\theta$  as shown in Figure 11.

Values of the matric flux potential,  $\phi$ , and the hydraulic conductivity,  $K(=\alpha\phi)$  are plotted in Figure 20 as a function of the relative depth,  $Z/L$ , for Treatment II. The matric flux potential and the hydraulic conductivity approach zero as  $Z$  goes to  $L$ . This is expected since the water application rate was taken equal to the water uptake rate. The matric flux potential and the hydraulic conductivity values generally increase near the plane source. Also, the small value of the matric flux potential at  $Z$  equal zero reveals a low evaporation potential of the soil surface under subsurface irrigation.

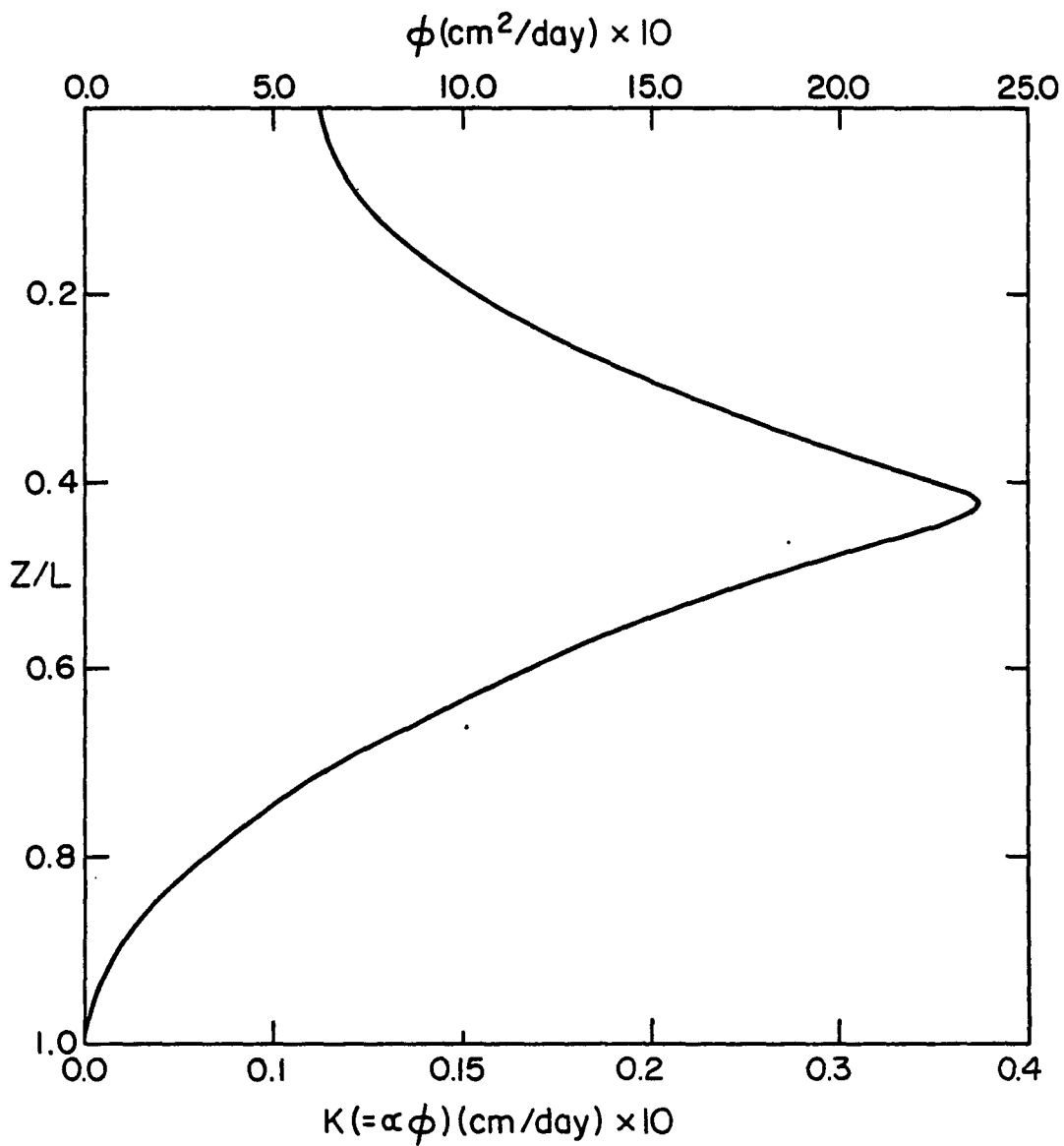


Figure 20. Profile of the Matric Flux Potential and Hydraulic Conductivity.

## CHAPTER 6

### TENSION IRRIGATION DESIGN CRITERIA

The design of a tension irrigation system can be based on the soil matric potential at any depth in the soil mass. However, the plane source depth, i.e.,  $Z$  equal  $d$ , seems to be the logical choice, because it is the easiest region of the soil mass to control the soil matric potential.

Values of a dimensionless matric flux potential,  $\phi_*$ , for  $Z$  equal  $d$  can be calculated from Eqs. (21) or (22) after dividing by  $aL/\alpha$ . Dimensionless matric flux potentials at depth  $d$  for six values of  $L$  are presented in Table 4.

The soil matric potential ( $h$ ) at the plane source depth can be computed by using the information in Table 4 and Eq. (23) if the irrigation rate ( $u = aL$ ), the root zone depth ( $L$ ), and the soil parameters  $\alpha$  and  $K_0$  are known. Values of  $K_0$  and  $\alpha$  for several soils can be obtained from Gilley and Allred (1972), Braester (1973), and Thomas et al. (1976).

#### Example 1

The following illustrates the procedure for determining the  $h$  value at  $Z$  equal  $d$ . The input parameters are given in Table 5. Solution: from Table 4, for  $L = 80$  cm,  $d = 30$  cm, and  $\alpha = 0.026$  cm<sup>-1</sup>, the value of  $\phi_*$  is between 0.268 and 0.301. A graphic interpolation would be

Table 4. Dimensionless Matric Flux Potential at Plane Source Depth.

Root Zone Depth L (cm)	Plane Source Depth d (cm)	Dimensionless Matric Flux Potential ( $\phi_* = \alpha\phi/aL$ )							
		$\alpha$ (cm <sup>-1</sup> )							
		0.010	0.015	0.020	0.025	0.030	0.035	0.040	0.050
40	10	0.102	0.146	0.186	0.222	0.255	0.285	0.313	0.361
	15	0.072	0.104	0.133	0.160	0.185	0.208	0.229	0.268
	20	0.047	0.068	0.088	0.106	0.124	0.140	0.155	0.183
50	15	0.109	0.155	0.196	0.233	0.266	0.296	0.323	0.369
	20	0.081	0.117	0.149	0.177	0.204	0.228	0.250	0.289
	25	0.057	0.083	0.106	0.128	0.148	0.166	0.183	0.214
60	20	0.117	0.165	0.208	0.245	0.278	0.307	0.334	0.378
	25	0.091	0.129	0.164	0.194	0.222	0.247	0.269	0.307
	30	0.068	0.097	0.124	0.148	0.170	0.190	0.208	0.241
80	25	0.158	0.219	0.270	0.313	0.350	0.382	0.409	0.453
	30	0.133	0.185	0.223	0.268	0.301	0.329	0.354	0.395
	35	0.109	0.153	0.191	0.224	0.253	0.279	0.301	0.338
100	30	0.196	0.266	0.323	0.369	0.407	0.438	0.465	0.506
	35	0.172	0.235	0.286	0.328	0.364	0.393	0.418	0.457
	40	0.149	0.204	0.250	0.289	0.321	0.349	0.372	0.410
120	35	0.231	0.308	0.368	0.414	0.452	0.482	0.507	0.544
	40	0.208	0.278	0.334	0.378	0.414	0.443	0.466	0.503
	50	0.164	0.222	0.269	0.307	0.339	0.365	0.387	0.421

Table 5. Input Parameters for Examples 1 and 2.

	Example 1	Example 2
Application rate ( $u = aL$ )	$0.6 \text{ cm day}^{-1}$	$0.5 \text{ cm day}^{-1}$
Root zone depth (L)	80 cm	80 cm
Source depth (d)	30 cm	30 cm
Hydraulic conductivity ( $K_0$ )	$2.52 \text{ cm day}^{-1}$	$1.0 \text{ cm day}^{-1}$
Alpha value ( $\alpha$ )	$0.026 \text{ cm}^{-1}$	-
Pressure head (h) at $Z = d$	-	-240 cm, $H_2O$

recommended since the  $\phi_*$  function is not linear. Interpolation yields  $\phi_* = 0.275$ . The matric flux potential is

$$\phi = \frac{\alpha L}{\alpha} \phi_* = \frac{0.6 \times 0.275}{0.026} \text{ cm}^2 \text{ day}^{-1} = 6.35 \text{ cm}^2 \text{ day}^{-1}$$

and from Eq. (23)

$$h = \frac{1}{\alpha} \ln \left( \frac{\alpha \phi}{K_o} \right) = \frac{1}{0.026 \text{ cm}^{-1}} \ln \left( \frac{6.35 \times 0.026}{2.52} \right) = -105 \text{ cm}$$

of water.

The predicted distribution of the soil matric potential,  $h$ , can be determined by Eq. (23), where the functions of  $\phi(Z)$  from Eqs. (21) and (22) are

$$\begin{aligned} \phi(Z) = & 23.1 \exp [0.026(Z - 30)] - 11.1(0.026Z - 1) \\ & + 11.1 \exp [0.026(Z - 80)] \end{aligned}$$

above the plane source ( $0 < Z < d$ ) and

$$\phi(Z) = 23.1 - 11.1(0.026Z - 1) + 11.1 \exp [0.026(Z - 80)]$$

below the plane source ( $d < Z < L$ ). A scientific calculator with memory capability is sufficient to calculate the values of  $\phi(Z)$  and  $h$ . The results are shown in Table 6.

For a given  $L$ , the values of the function  $\phi(Z)$  are highly sensitive to  $\alpha$ . As shown in Chapter 5, the values of  $\alpha$  used in the mathematical model that best predicted the measured values of the matric potential

Table 6. Values of the Matric Flux Potential and Pressure Head versus Depth for Example 1.

Z (cm)	$\phi(Z)$ (cm <sup>2</sup> /day)	h (-cm of water)
0	0.870	181
5	1.089	173
10	1.538	159
20	3.261	130
30	6.352	105
40	4.365	119
50	2.645	138
60	1.271	167
70	0.344	217
75	0.090	268

decreased from  $0.026 \text{ cm}^{-1}$  (when  $h = -151 \text{ cm}$  of water) to  $0.0117 \text{ cm}^{-1}$  (when  $h = -341 \text{ cm}$  of water) for the Pima clay loam soil. Also, because of the completely unsaturated nature of the moisture flow with a tension irrigation system, the value of  $K_o$  in Eq. (23) should be interpreted as an empirical constant and not as the saturated hydraulic conductivity of the soil.

### Example 2

If the hydraulic conductivity of the soil for a given value of  $h$  is known, Table 4 can be used to estimate the value of  $\alpha$  in Eq. (23) that will match with the  $h$  value at the plane source depth. The procedure is trial and error. For the input parameters in Table 5, the solution is:

1. First trial,  $\alpha = 0.01 \text{ cm}^{-1}$ . For this  $\alpha$  value,  $L = 80 \text{ cm}$  and  $d = 30 \text{ cm}$ ,  $\phi_* = 0.133$ , from Table 4.

$$\phi = \frac{\alpha L}{\alpha} \phi_* = \frac{0.5 \text{ cm day}^{-1}}{0.01 \text{ cm}^{-1}} \times 0.133 = 6.66 \text{ cm}^2 \text{ day}^{-1}$$

and from Eq. (23)

$$h = \frac{1}{\alpha} \ln \left( \frac{\alpha \phi}{K_o} \right) = \frac{1}{0.01 \text{ cm}^{-1}} \ln \left( \frac{0.01 \times 6.66}{1} \right) = -271 \text{ cm}$$

of water which is low compared with  $-240 \text{ cm}$ .

2. Second trial,  $\alpha = 0.012 \text{ cm}^{-1}$ . From Table 4, after interpolation,  $\phi_* = 0.155$  and

$$\phi = \frac{aL}{\alpha} = \frac{.5 \text{ cm day}^{-1}}{0.012 \text{ cm}^{-1}} \times 0.155 = 6.46 \text{ cm}^2 \text{ day}^{-1}$$

$$h = \frac{1}{\alpha} \ln \left( \frac{\alpha\phi}{K_o} \right) = \frac{1}{0.012 \text{ cm}^{-1}} \ln \left( \frac{0.012 \times 6.46}{1} \right) = -213 \text{ cm}$$

of water, which is high.

3. Third trial,  $\alpha = 0.011 \text{ cm}^{-1}$ . From Table 4,  $\phi_* = .145$  (by interpolation)

$$\phi = \frac{aL}{\alpha} = \frac{.5 \text{ cm day}^{-1}}{0.011 \text{ cm}^{-1}} \times 0.145 = 6.59 \text{ cm}^2 \text{ day}^{-1}$$

$$h = \frac{1}{\alpha} \ln \left( \frac{\alpha\phi}{K_o} \right) = \frac{1}{0.011 \text{ cm}^{-1}} \ln \left( \frac{0.011 \times 6.59}{1} \right) = -239 \text{ cm}$$

of water, which is sufficiently close to the given value of -240 cm.

The soil matric potential versus depth can then be calculated from Eq. (23) after the values of the function  $\phi(Z)$  are calculated from Eqs. (21) and (22) as the first example.

#### Placement of the Line Sources

A series of parallel line sources (ceramic tubes) can simulate a plane source when they are placed sufficiently close together. The distribution patterns for matric flux potential as a function of spacing can be studied using a two-dimensional analysis of the moisture flow equation. The matric flux potential for a single line source at depth D is (Raats, 1972, Eq. 11):

$$\phi_L(X,Z) = (q/2\pi) \{ \phi_\infty(X,Z-D) + \exp(-2D) \phi_\infty(X,Z+D) - 2 \exp(2Z) \int_{Z+D}^{\infty} \exp(-2t) \phi_\infty(X,t) dt \} \quad (28)$$

where  $q$  is the flux (units  $L^2/T$ ),  $X = \alpha x/2$ ,  $Z = \alpha z/2$ ,  $D = \alpha d/2$ , with  $x$ ,  $z$ , and  $d$  as real coordinates and depth. The  $\phi_\infty$  is the matric flux of a line source in an infinite medium (Philip, 1968, 1971):

$$\phi_\infty(X,Z) = (q/2\pi) \exp(Z) K_0 [(X^2 + Z^2)^{1/2}] \quad (29)$$

In Eq. (29),  $K_0$  is a modified Bessel function of the second kind of order zero. The solution for an infinite number of parallel line sources located at  $X_1, X_2, \dots, X_j$ , is (Lomen and Warrick, 1974, Eq. 21)

$$\sum_{j=1}^{\infty} \phi_L(X - X_j, Z, T) \quad (30)$$

These solutions were used to compute the distribution of the matric flux potentials,  $\phi$  (units  $L^2/T$ ), shown in Figure 21. The spacing between lines was 30 cm and the input parameters were those in Table 5, Example 2. From this flow pattern (no sink term added), one observes the horizontal component of the moisture flow 10 cm above or 20 cm below the sources are negligible, that is, the flow is nearly one-dimensional upward and downward from these depths, respectively.

Profiles of the matric flux potentials,  $\phi$ , and pressure head,  $h$ , midway between two consecutive line sources 0.0, 30.0, 60.0, and 90.0 cm

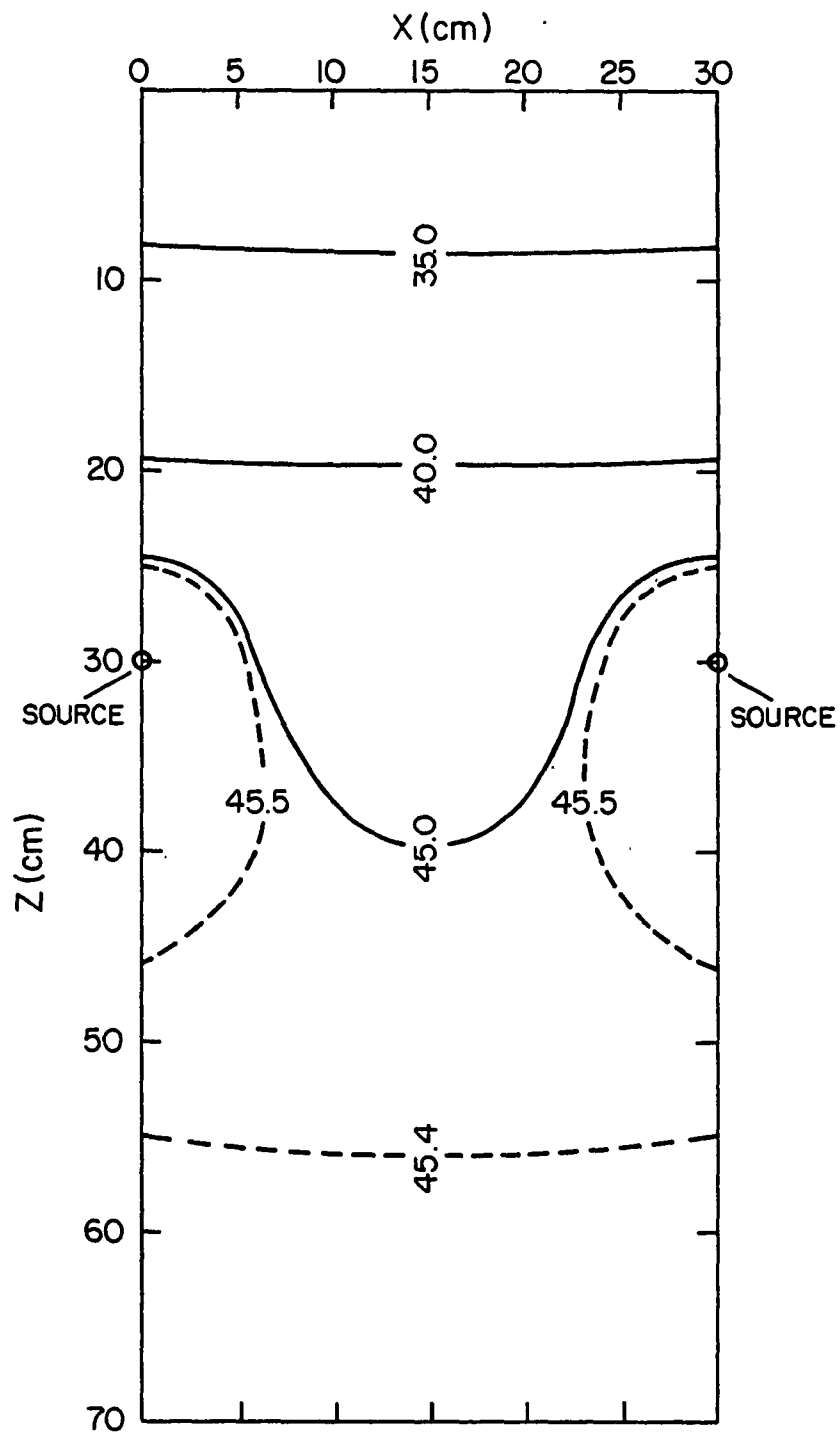


Figure 21. Two-Dimensional Matrix Flux Potential Distribution without Sink.

apart are presented in Figure 22. Values were calculated using the water added per unit surface area  $u = 0.5 \text{ cm day}^{-1}$  for each case. Thus, the wider spacings are compensated for by higher discharge rates from the lines. From these curves, one can see that, as spacing increases, the deviation from the one-dimensional flow increases. For example,  $\phi$  values at the source depth decrease from 45.5 (one-dimensional) to 43.8, 42.1, and  $40.4 \text{ cm}^2 \text{ day}^{-1}$  for the 30.0, 60.0, and 90.0 cm spacing, respectively. In addition, Figure 22 shows that, for shallow rooting depths, the line sources should be placed closer together than for deeper ones, if the one-dimensional model were used. The values of matric flux potential  $\phi(X_m, Z)$  midway between lines were subtracted from the values of  $\phi_s(Z)$  (sink) of Eq. (10) and plotted as Figure 23. Values of the matric potential,  $h$ , can also be read directly. The matric potential values greatly decrease with increasing spacing. For example,  $h$  values at the source depth change from -240 (one-dimensional) to -266, -303, and -372 cm of water for the 30, 60, and 90 cm spacing, respectively.

This analysis has shown that the one-dimensional model can be used in the design of a tension irrigation system. However, the line sources should be placed sufficiently close together, in which case, the flux can be considered one-dimensional except near the depth of the tubes.

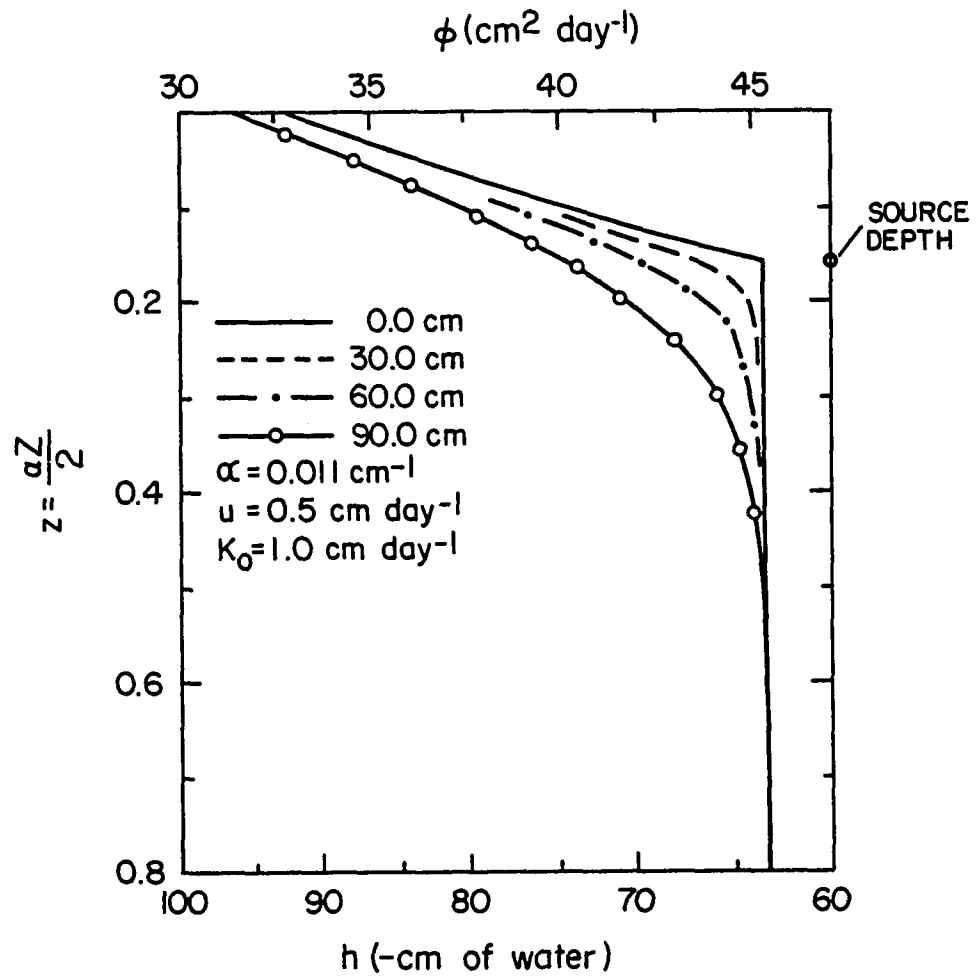


Figure 22. Predicted Matric Flux Potential and Pressure Head without Sink.

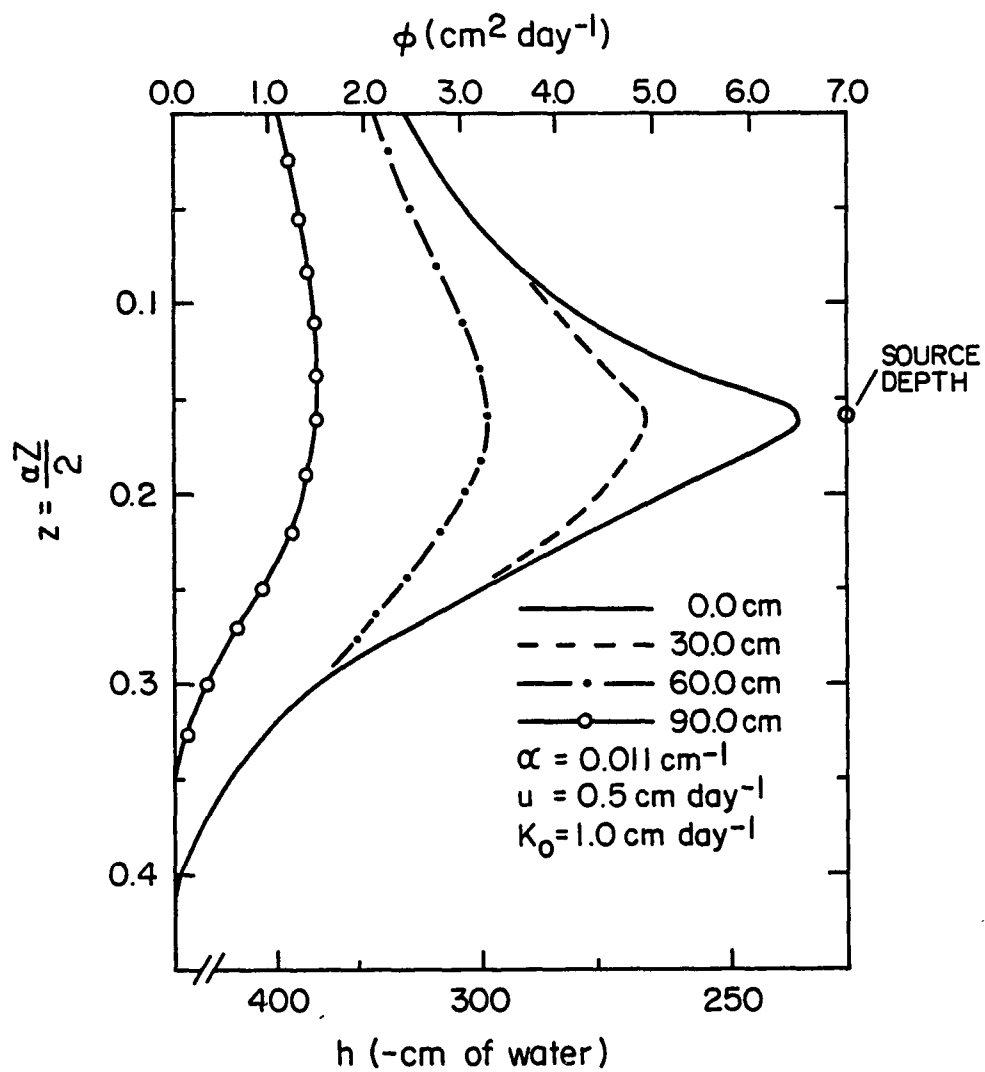


Figure 23. Predicted Matric Flux Potential and Pressure Head with Sink.

## CHAPTER 7

### SUMMARY AND CONCLUSIONS

Lettuce was raised in a greenhouse during the Fall and Winter seasons of 1976-1977 under controlled soil matric potentials, using a tension irrigation system. The tension irrigation system consisted of a soil bin (45 cm deep, 55 cm long, and 30.5 cm wide) and buried ceramic tubes connected to a negative head water delivery system by plastic tubes. Soil moisture tension was measured at the 8, 18, 29, and 39 cm depths. Air temperature and relative humidity were continuously recorded by a hygrothermograph placed near the soil bins.

The soil was a Pima clay loam obtained from the University of Arizona experimental farm at Marana. Superphosphate was mixed with the soil before filling the soil bin to provide 140 ppm dry weight of  $P_2O_5$ . Lettuce plants were thinned to two plants per soil bin. Two applications of 20 ppm of nitrogen (4 gm of urea per soil bin) with the irrigation water were made 15 and 55 days after germination. Consumptive use of water by lettuce was measured by direct readings from the water delivery system reservoir.

Evapotranspiration rate for the Fall experiment increased during the first 50 days of growth, corresponding to the increase in leaf area. Maximum values recorded were 4.2 mm/day. The evapotranspiration rates decreased in the later period of growth because of cold weather and short day lengths. Variation of the daily evapotranspiration indicated

sensitivity of the tension irrigation system for meeting the consumptive use of water by plants. The total water used was 240 mm (9.4 inches).

The Winter experiment consisted of three soil water treatments: Treatment I, -10 to -15 cbars soil water potential during the growing season; Treatment II, -10 to -15 cbars during the first 45 days of growth and then -20 to -25 cbars; and Treatment III, -10 to -15 cbars during the first 45 days of growth and then -30 to -35 cbars. The three treatments had similar evapotranspiration rates during the first 45 days of the growing season. With adjustment of the soil water tension, a tendency of increasing evapotranspiration values at lower soil moisture tension was observed. For example, Treatment I reached an evapotranspiration rate of 7.0 mm/day compared with the 4.4 mm/day maximum of Treatment III. The totals of water used were 206 mm (8.1 in.), 188 mm (7.4 in.), and 174 mm (6.8 in.) for Treatments I, II, and III, respectively.

A one-dimensional soil-moisture model was developed, and measured values of the soil matric potentials were compared with predicted values. For the Fall experiment, an adequate agreement between calculated and measured soil-water potential was achieved by assuming 60 percent of the water was withdrawn from the top 22 cm of the root zone and 40 percent withdrawn below 22 cm. Calculated soil matric potentials were within 12 percent of the measured values.

A uniform water withdrawal pattern by the plants resulted in good agreement between measured and computed soil matric potentials for the Winter experiment. Exceptions were the 29 cm depth of Treatments II and III and the 39 cm depth of Treatment I where the calculated capillary

potential values were within 21 percent of the measured values. High root density just below the plane source and poor simulation of the lower boundary condition by the mathematical model were assumed to be the main reasons for the poor agreement at these points.

The matric flux potential was highest near the plane source and decreased with distance both above and below. The low values of the matric flux potential at the soil surface revealed a low evaporation potential at the soil surface under subsurface irrigation. Tension irrigation system design criteria based on the values of the dimensionless matric flux potential at the plane source depth were presented.

The results of this investigation led to the following conclusions:

1. A tension irrigation system can be used to measure water use by crops under controlled soil matric potentials.
2. Peak evapotranspiration rates and total consumptive use of water by lettuce increase with increasing soil matric potential in the range studied. However, soil-water potentials greater than -30 cbars appeared to decrease lettuce yield, possibly because of poor soil aeration.
3. The control of the soil matric potentials away from the source using tension irrigation system was better for the wetter than for the drier soil moisture levels.
4. Calculated soil matric potentials using a mathematical model closely predicted measured values. The model can be used as a tool for tension irrigation design.

The primary effort of the study was to determine the basic factors that affect the performance and usefulness of a tension irrigation system as a tool in research on consumptive use of water by plants and plant response under controlled soil matric potentials. Further investigations using different crops, soil volumes, and soil types would be of interest.

APPENDIX

MEASURED VALUES OF EVAPOTRANSPIRATION AND SOIL MATRIC  
POTENTIALS FOR THE FALL AND WINTER EXPERIMENTS

Table A1. Measured Values of Evapotranspiration and Soil Matric Potentials for the Fall Experiment.

Date 1976-77	Negative Head (cm H <sub>2</sub> O)	Evapotranspiration		Soil Matric Potentials (cbars)			
		Eta (mm/day)	ΣEta (mm)	Tensiometer Depth (cm)			
				8	18	29	39
Sep. 25	118	-	-	15	15	14	15
30	"	1.20	6.00	16	16	15	15
Oct. 5	"	1.47	13.37	16	17	16	16
10	"	1.90	22.88	17	16	16	17
14	"	2.20	30.95	19	15	17	16
15	"	2.23	33.18	18	15	14	18
16	"	2.13	35.31	20	14	13	17
17	"	2.43	37.74	20	16	15	18
18	"	2.17	39.91	20	15	14	17
19	"	2.37	42.28	20	14	13	17
20	"	2.19	44.47	20	15	15	18
21	"	2.43	46.90	20	15	14	17
22	"	2.32	49.22	20	15	14	17
23	"	2.30	51.52	18	16	16	18
24	"	2.22	53.74	20	15	14	18
25	"	2.13	55.87	21	15	14	17
26	"	2.23	58.10	22	15	15	18
27	"	2.33	60.43	21	16	15	19
28	"	2.39	62.82	22	16	15	19
29	"	2.33	65.15	22	18	17	20
30	"	2.39	67.54	23	18	17	21
31	"	2.86	70.40	25	17	17	21
Nov. 1	"	2.75	73.15	26	19	19	22
2	"	2.95	76.10	28	19	20	22
3	"	3.50	79.60	32	21	21	23
4	"	3.50	83.10	34	23	24	27
5	"	3.79	86.89	37	25	26	30
6	"	4.05	90.94	45	25	28	31
7	"	3.96	94.90	47	30	33	36
8	"	4.00	98.90	49	31	36	38
9	"	4.23	103.13	51	35	40	42
10	"	4.10	107.23	53	35	44	46
11	"	4.00	111.23	57	36	48	52
12	99	4.26	115.49	58	38	54	57
13	"	4.40	119.89	58	34	51	58
14	"	2.48	122.37	48	33	51	59
15	"	3.50	125.87	48	33	53	61
16	"	3.46	129.33	53	33	53	63
17	"	3.55	132.88	50	35	55	57

Table A1, Continued.

Date 1976-77	Negative Head (cm H <sub>2</sub> O)	Evapotranspiration		Soil Matric Potentials (cbars)			
		Eta (mm/day)	ΣEta (mm)	Tensiometer Depth (cm)			
				8	18	29	39
Nov. 18	78	3.73	136.61	50	55	56	57
19	"	4.32	140.92	51	31	53	61
20	"	4.16	145.09	48	30	53	61
21	"	4.29	149.38	47	29	52	61
22	"	4.08	153.46	46	30	53	65
23	"	4.29	157.75	45	31	55	69
24	"	4.19	161.94	48	32	55	69
25	"	4.09	166.03	45	32	54	69
26	"	3.88	169.91	45	34	54	70
27	"	3.99	173.90	46	35	56	70
28	"	2.97	176.87	44	34	55	68
29	"	2.97	179.84	44	35	53	66
30	"	2.92	182.76	41	33	52	64
Dec. 1	"	2.97	185.73	43	34	53	64
2	"	3.22	188.95	42	35	53	63
3	59	3.16	192.11	44	38	55	63
4	"	3.73	195.84	43	35	55	63
5	"	3.51	199.35	41	35	54	62
6	"	3.23	202.58	41	35	54	61
7	"	3.13	205.71	39	34	51	60
8	"	2.95	208.66	40	35	52	60
9	"	2.80	211.46	41	35	52	60
10	"	3.05	214.51	40	33	49	58
11	"	2.77	217.28	40	33	50	58
12	"	2.62	219.90	39	33	49	57
13	"	2.95	222.85	38	32	47	55
14	"	2.83	225.68	40	32	48	55
15	"	2.62	228.30	41	33	48	55
16	"	2.67	230.97	38	32	47	54
17	"	2.63	233.60	41	33	48	54
18	"	2.62	236.22	41	31	48	52
19	"	2.80	239.02	40	31	46	52
20	"	2.22	241.24	38	29	44	51

Table A2. Measured Values of Evapotranspiration and Soil Matric Potentials for the Winter Experiment -- Treatment I.

Date 1976-77	Negative Head (cm H <sub>2</sub> O)	Evapotranspiration		Soil Matric Potentials (cbars)			
		Eta (mm/day)	ΣEta (mm)	Tensiometer Depth (cm)			
				8	18	29	39
Nov. 25	118	.80	4.00	12	11	12	12
30	"	.71	8.26	13	12	12	13
Dec. 6	"	.83	12.41	13	11	11	12
11	"	.91	16.96	13	12	13	13
16	"	1.04	22.16	13	12	14	13
21	"	1.17	28.01	14	12	14	13
26	"	1.42	35.11	14	13	14	13
31	"	1.74	42.07	14	14	14	14
Jan. 4	"	1.97	44.04	18	15	17	17
5	"	1.54	45.58	16	14	16	15
6	100	2.39	47.97	17	15	16	16
7	"	2.36	50.33	17	14	15	16
8	"	1.60	51.93	17	14	15	16
9	"	1.60	51.93	14	13	15	15
10	"	1.67	53.60	16	13	13	15
11	"	2.04	55.64	16	13	14	16
12	"	2.32	57.96	17	14	15	16
13	"	2.49	60.45	17	15	16	17
14	"	2.62	63.07	18	15	16	17
15	80	2.92	55.99	19	16	18	19
16	"	4.20	70.19	18	15	18	19
17	"	3.80	73.99	18	14	17	19
18	"	3.40	77.39	20	15	18	20
19	"	3.58	80.97	19	15	20	21
20	60	4.29	85.26	20	15	21	22
21	"	3.95	89.21	19	15	19	20
22	"	2.93	92.14	18	14	19	20
23	"	2.40	94.54	17	15	20	21
24	45	3.12	97.66	18	15	20	21
25	"	3.49	101.15	19	17	22	23
26	"	3.88	105.03	19	16	22	24
27	"	4.10	109.13	18	15	22	23
28	"	4.60	113.73	18	15	24	25
29	"	5.20	118.93	17	14	23	24
30	"	4.66	123.59	15	13	21	23
Jan. 31	45	2.53	126.12	15	13	20	22
Feb. 1	"	3.41	129.53	16	14	22	23
2	31	4.49	134.02	17	15	22	24
3	"	4.15	138.17	19	15	23	28

Table A2, Continued.

Date 1976-77	Negative Head (cm H <sub>2</sub> O)	<u>Evapotranspiration</u>		<u>Soil Matric Potentials (cbars)</u> <u>Tensiometer Depth (cm)</u>			
		<u>Eta</u> (mm/day)	<u>ΣEta</u> (mm)	8	18	29	39
Feb. 4	31	5.02	143.19	18	14	25	30
5	"	5.09	148.28	19	15	28	33
6	"	5.52	153.80	20	16	31	35
7	25	6.43	160.26	18	16	31	36
8	"	7.08	167.34	16	14	30	33
9	"	6.88	174.22	17	13	29	33
10	"	6.97	181.19	16	12	28	33
11	"	6.48	187.67	16	12	27	32
12	"	6.25	193.92	15	13	27	33
13	"	6.01	199.93	17	14	28	32
14	"	6.29	206.22	16	15	29	13

Table A3. Measured Values of Evapotranspiration and Soil Matric Potentials for the Winter Experiment -- Treatment II.

Date 1976-77	Negative Head (cm H <sub>2</sub> O)	Evapotranspiration		Soil Matric Potentials (cbars)			
		Eta (mm/day)	ΣEta (mm)	Tensiometer Depth (cm)			
				8	18	29	39
Nov. 25	118	-	-	11	12	13	12
30	"	.58	2.90	12	13	14	14
Dec. 6	"	.68	6.98	12	13	14	13
11	"	.91	11.53	13	14	16	15
16	"	1.09	16.98	14	14	18	18
21	"	1.17	22.83	19	17	19	21
26	"	1.23	28.98	24	19	22	23
31	"	1.29	35.43	27	22	23	25
Jan. 4	"	1.66	42.07	30	24	26	28
5	"	1.76	43.83	31	23	27	28
6	110	1.60	45.43	33	25	27	29
7	"	2.10	47.53	35	25	26	28
8	"	2.26	49.79	33	24	26	28
9	"	1.96	51.75	30	23	27	30
10	"	1.92	53.67	30	24	28	30
11	80	2.36	56.03	33	25	30	32
12	"	2.37	58.40	33	25	30	32
13	"	2.67	61.07	35	26	32	33
14	59	3.05	64.12	37	26	32	34
15	41	3.52	67.64	37	26	33	36
16	"	4.29	71.93	31	22	31	34
17	"	4.23	76.16	29	22	34	37
18	"	3.76	79.92	28	23	33	37
19	"	3.76	83.68	29	24	35	39
20	"	4.48	88.16	28	25	35	40
21	"	3.72	91.88	21	24	34	39
22	"	3.30	95.18	26	24	35	39
23	"	2.43	97.61	27	25	35	40
24	"	2.83	100.44	27	25	36	40
25	"	3.27	103.71	27	26	37	43
26	35	3.45	107.16	28	26	38	43
27	"	3.86	111.02	26	24	37	45
28	"	4.08	115.00	24	22	35	45
29	"	4.75	119.85	23	20	34	43
30	30	3.35	123.20	22	20	30	42
31	"	2.74	125.94	21	19	28	42
Feb. 1	"	3.62	129.56	22	21	32	43
2	"	4.13	133.69	25	23	35	46
3	"	3.93	137.62	25	24	36	48

Table A3, Continued.

Date 1976-77	Negative Head (cm H <sub>2</sub> O)	Evapotranspiration		Soil Matric Potentials (cbars)			
		Eta (mm/day)	ΣEta (mm)	Tensiometer Depth (cm)			
				8	18	29	39
Feb. 4	30	4.00	141.62	26	25	37	52
5	"	4.29	145.91	25	25	42	55
6	21	4.43	150.34	26	26	44	55
7	"	4.75	155.09	25	23	46	54
8	"	4.85	159.94	24	22	45	54
9	"	4.59	164.53	25	23	47	55
10	"	4.75	169.28	26	24	47	57
11	"	4.66	173.94	24	23	46	57
12	"	4.59	178.53	24	23	47	56
13	"	4.53	183.06	24	22	47	55
14	"	4.59	187.65	25	23	48	56

Table A4. Measured Values of Evapotranspiration and Soil Matric Potentials for the Winter Experiment -- Treatment III.

Date 1976-77	Negative Head (cm H <sub>2</sub> O)	Evapotranspiration		Soil Matric Potentials (cbars)			
		Eta (mm/day)	ΣEta (mm)	Tensiometer Depth (cm)			
				8	18	29	39
Nov. 25	118	-	-	11	12	10	12
30	"	.53	2.65	12	12	10	14
Dec. 6	"	.79	7.39	12	12	10	13
11	"	.93	12.04	13	13	12	14
16	177	1.00	17.04	13	13	12	15
21	"	1.04	22.24	19	17	17	18
26	"	1.17	28.09	24	21	20	24
31	"	1.11	33.64	29	26	25	27
Jan. 4	"	1.39	39.20	36	30	30	31
5	"	1.41	40.61	35	31	32	31
6	"	1.26	41.87	40	33	33	33
7	136	1.57	43.44	41	35	35	36
8	"	1.59	45.03	43	35	35	36
9	"	1.43	46.46	39	34	36	38
10	100	1.40	47.86	42	36	37	40
11	"	2.04	49.90	40	36	40	43
12	80	2.37	52.27	41	36	40	43
13	59	2.43	54.70	41	37	42	44
14	"	2.92	57.62	37	33	42	48
15	"	3.89	61.51	36	32	45	51
16	"	4.15	65.66	38	34	44	53
17	40	3.70	69.36	38	35	45	55
18	"	3.58	72.94	37	34	45	58
19	30	3.88	76.82	37	35	47	61
20	"	4.23	81.05	37	34	46	65
21	"	3.76	84.81	36	33	47	65
22	"	3.17	87.98	36	31	47	65
23	"	2.27	90.25	37	32	46	67
24	"	2.66	92.91	39	34	48	67
25	20	3.20	96.11	39	35	49	68
26	"	3.60	99.71	37	33	51	69
27	"	3.80	103.51	35	30	51	70
28	"	4.00	107.51	35	32	52	71
29	"	4.40	111.91	36	32	53	71
30	"	3.00	114.91	35	32	55	72
31	"	2.39	117.30	35	33	56	72
Feb. 1	"	3.27	120.57	35	33	55	74
2	"	4.30	124.87	36	34	56	76

Table A4, Continued.

Date 1976-77	Negative Head (cm H <sub>2</sub> O)	Evapotranspiration		Soil Matric Potentials (cbars)			
		Eta (mm/day)	ΣEta (mm)	Tensiometer Depth (cm)			
				8	18	29	39
Feb. 3	20	3.78	128.65	37	35	56	76
4	15	3.86	132.51	39	37	57	78
5	"	4.09	136.60	37	33	57	81
6	"	4.22	140.82	35	31	55	80
7	"	4.40	145.22	35	30	55	80
8	"	4.33	149.55	38	34	58	81
9	"	4.17	153.72	38	35	58	81
10	"	4.40	158.12	40	37	60	82
11	"	4.20	162.32	39	35	59	82
12	"	4.00	166.32	37	33	57	81
13	"	3.70	170.02	37	34	58	80
14	"	3.89	173.91	36	33	56	80

## LITERATURE CITED

- Braester, C. 1973. Moisture variation at the soil surface and the advance of the wetting front during infiltration at constant flux. Water Resour. Res., 9: 687-694.
- Brandt, A., E. Bresler, N. Diner, I. Ben-Asher, J. Heller, and D. Goldberg. 1971. Infiltration from a trickle source: I. Mathematical models. Soil Sci. Soc. Amer. Proc., 35: 675-682.
- Bresler, E., J. Heller, N. Diner, I. Ben-Asher, A. Brandt, and D. Goldberg. 1971. Infiltration from a trickle source: II. Experimental data and theoretical predictions. Soil Sci. Soc. Amer. Proc., 35: 683-689.
- Brust, K. J., C. H. M. Van Bavel, and G. B. Stirk. 1968. Hydraulic properties of a clay loam soil and the field measurement of water uptake by plants: III. Comparison of field and laboratory data on retention and of measured and calculated conductivities. Soil Sci. Soc. Amer. Proc., 32: 322-326.
- Childs, E. C., and N. Collis-George. 1950. The permeability of porous materials. Proc. Roy. Soc., A201: 392-405.
- Erie, L. J., O. F. French, and K. Harris. 1968. Consumptive use of water by crops in Arizona. Ariz. Agr. Exp. Sta. Bull. 169.
- Gardner, W. R. 1958. Some steady-state solutions of the unsaturated moisture-flow equation with application to evaporation from a water table. Soil Sci., 85: 228-232.
- Gilley, J. R., and E. R. Allred. 1972. Infiltration and root extraction from subsurface irrigation laterals. ASAE Paper 72-743, Amer. Soc. Agric. Engr. (St. Joseph, Michigan).
- Hendrickson, A. H., and F. J. Veihmeyer. 1931. Influence of dry soil on root extension. Plant Physiol., 6: 567-576.
- Hillel, D. 1971. Soil and Water Physical Principles and Processes. New York: Academic Press. 288 p.
- Jackson, R. D., R. J. Reginato, and C. H. M. Van Bavel. 1965. Comparison of measured and calculated hydraulic conductivities of unsaturated soils. Water Resour. Res., 1: 375-379.

- Knott, J. E., E. M. Andersen, and R. D. Sweet. 1939. Problems in the production of iceberg lettuce in New York. Agr. Exp. Sta. Bull., 714: 1-17.
- Kunze, R. J., G. Uehara, and K. Graham. 1968. Factors important in the calculation of hydraulic conductivity. Soil Sci. Soc. Amer. Proc., 32: 760-765.
- Livingston, B. E. 1908. A method for controlling plant moisture. Plant World, 11: 39-40.
- \_\_\_\_\_. 1918. Porous clay cones for the auto-irrigation of potted plants. Plant World, 21: 202-208.
- Livingston, B. E., T. Hemmi, and J. D. Wilson. 1926. Growth of young wheat plants in auto-irrigated soils as related to the water-supplying power of the soil and to the adjustment of the auto-irrigator. Plant Physiol., 1: 387-395.
- Lomen, D. O., and A. W. Warrick. 1974. Time-dependent linearized infiltration: II. Line sources. Soil Sci. Soc. Amer. Proc., 38: 568-572.
- Marshall, T. J. 1958. A relation between permeability and size distribution of pores. J. Soil Sci., 9: 1-8.
- Millington, R. J., and J. P. Quirk. 1959. Permeability of porous media. Nature, 183: 387-388.
- \_\_\_\_\_. 1960. Transport in porous media. Int. Congr. Soil Sci., Trans. 7th (Madison, Wisconsin), 1.3: 97-106.
- \_\_\_\_\_. 1961. Permeability of porous solids. Trans. Faraday Soc., 57: 1,200-1,207.
- Moore, F. D., and P. N. Soltanpour. 1972. Evapotranspiration of head lettuce: An estimate for June planting in the San Luis Valley. Col. Agr. Exp. Sta. Bull. 113.
- Moore, R. E. 1939. Water conduction from shallow water tables. Hilgardia, 12: 383-426.
- Nimah, M. N., and R. J. Hanks. 1973a. Model for estimating soil water, plant, and atmospheric interrelations: I. Description and sensitivity. Soil Sci. Soc. Amer. Proc., 37: 522-527.
- \_\_\_\_\_. 1973b. Model for estimating soil water, plant, and atmospheric interrelations: II. Field test of model. Soil Sci. Soc. Amer. Proc., 37: 528-534.

- Pereira, O. J. 1971. Mapping and characterization of the soils on the University of Arizona experimental farm at Marana. M. S. Thesis, University of Arizona, Tucson.
- Philip, J. R. 1957. The physical principles of soil water movement during the irrigation cycle. Proc. Intern. Congr. Irrigation Drainage, 3rd (San Francisco, California), pp. 8.125-8.154.
- \_\_\_\_\_. 1968. Steady infiltration from buried point sources and spherical cavities. Water Resour. Res., 4: 1039-1047.
- \_\_\_\_\_. 1969. Theory of infiltration. Advan. Hydrosci., 5: 215-296.
- \_\_\_\_\_. 1971. General theorem on steady infiltration from surface sources, with application to point and line sources. Soil Sci. Soc. Amer. Proc., 35: 867-871.
- Raats, P. A. C. 1970. Steady infiltration from line sources and furrows. Soil Sci. Soc. Amer. Proc., 34: 709-714.
- \_\_\_\_\_. 1971. Steady infiltration from point sources, cavities and basins. Soil Sci. Soc. Amer. Proc., 35: 689-694.
- \_\_\_\_\_. 1972. Steady infiltration from sources at arbitrary depth. Soil Sci. Soc. Amer. Proc., 36: 399-401.
- Read, D. W. L., S. V. Fleck, and W. L. Pelton. 1962. Self-irrigating green house pots. Agron. J., 54: 467-468.
- Remson, I., and G. S. Fox. 1955. Capillary losses from ground water. Trans. Amer. Geophys. Union, 36: 304-310.
- Richards, L. A. 1931. Capillary conduction of liquids through porous mediums. Physics, 1: 318-333.
- Richards, L. A., and H. L. Blood. 1934. Some improvements in auto-irrigator apparatus. J. Agr. Res., 49: 115-121.
- Richards, L. A., and W. E. Loomis. 1942. Limitations of auto-irrigators for controlling soil moisture under growing plants. Plant Physiol., 17: 223-235.
- Robinson, F. 1970. Population density and growth rate of head lettuce (*Lactuca sativa* L.) in an arid climate with sprinkler irrigation. J. Amer. Soc. Hort. Sci., 95: 831-834.
- Schwalen, H. C., and M. F. Wharton. 1930. Lettuce irrigation studies. Ariz. Agr. Exp. Sta. Bull., 133: 463-517.

- Soil Survey Staff. 1975. Soil Taxonomy, A Basic System of Soil Classification for Making and Interpreting Soil Surveys, U. S. Department of Agriculture Handbook No. 436. Washington, D. C.: U. S. Government Printing Office.
- Stanhill, G. 1957. The effect of differences in soil-moisture status on plant growth: A review and analysis of soil moisture regime experiments. Soil Sci., 84: 205-214.
- Taylor, S. A., and G. L. Ashcroft. 1972. Physical Edaphology. San Francisco: W. H. Freeman and Co. 533 p.
- Thomas, A. W., H. R. Duke, D. W. Zachmann, and E. G. Kruse. 1976. Comparison of calculated and measured capillary potentials from line sources. Soil Sci. Soc. Amer. J., 40: 10-14.
- Veihmeyer, F. J., and A. H. Holland. 1949. Irrigation and cultivation of lettuce. Calif. Agr. Exp. Sta. Bull. 711.
- Warrick, A. W. 1974a. Time-dependent linearized infiltration: I. Point sources. Soil Sci. Soc. Amer. Proc., 38: 383-386.
- \_\_\_\_\_. 1974b. Solution to the one-dimensional linear moisture flow equation with water extraction. Soil Sci. Soc. Amer. Proc., 38: 573-576.
- Watson, K. K. 1974. Some applications of unsaturated flow theory. In J. Van Schilfgaard (ed.), Drainage for Agriculture, pp. 359-400.
- Wharton, M. F., and C. Hobart. 1931. Studies in lettuce seedbed irrigation under high temperature conditions. Ariz. Agr. Exp. Sta. Bull. 33.
- Whitaker, T. W., E. J. Ryder, V. E. Rubatsky, and P. V. Vail. 1974. Lettuce production in the United States. U. S. Dept. Agr., Agr. Res. Serv. Handbook 221.
- Wilson, J. D. 1929. A double-walled pot for the auto-irrigation of plants. Bull. Torrey Bot. Club, 56: 139-153.
- Wooding, R. A. 1968. Steady infiltration from a circular pond. Water Resour. Res., 4: 1259-1273.